

Behaviour and neuropathology in mice injected with human contactin-associated protein 2 antibodies

Journal:	<i>Brain</i>
Manuscript ID	BRAIN-2018-01490.R1
Manuscript Type:	Original Article
Date Submitted by the Author:	21-Jan-2019
Complete List of Authors:	<p>Giannoccaro, Maria; University of Oxford, Nuffield Dept of Clinical Neurosciences; IRCSS, Istituto delle Scienze Neurologiche di Bologna, Department of Neurological Sciences, University of Bologna</p> <p>Menassa, David; University of Oxford, Nuffield Dept of Clinical Neurosciences; 3 Biological Sciences, University of Southampton, Southampton, UK</p> <p>Jacobson, Leslie; University of Oxford, Nuffield Department of Clinical Neurosciences</p> <p>Coutinho, Ester; University of Oxford, Nuffield Dept of Clinical Neurosciences</p> <p>Prota, Gennaro; MRC Human Immunology Unit, Weatherall Institute of Molecular Medicine, John Radcliffe Hospital, University of Oxford, Oxford, UK.</p> <p>Lang, Bethan; University of Oxford,</p> <p>Leite, M Isabel; University of Oxford, Nuffield Dept of Clinical Neurosciences</p> <p>Cerundolo, Vincenzo; MRC Human Immunology Unit, Weatherall Institute of Molecular Medicine, John Radcliffe Hospital, University of Oxford, Oxford, UK.</p> <p>Liguori, Rocco; IRCSS, Istituto delle Scienze Neurologiche di Bologna, Department of Neurological Sciences, University of Bologna; Department of Biomedical and Neuromotor Sciences, University of Bologna, Bologna, Italy</p> <p>Vincent, Angela; University of Oxford, Nuffield Dept of Clinical Neurosciences</p>
Subject category:	Multiple sclerosis and neuroinflammation
To search keyword list, use whole or part words followed by an *:	<p>Encephalitis < MULTIPLE SCLEROSIS AND NEUROINFLAMMATION, Limbic encephalitis < MULTIPLE SCLEROSIS AND NEUROINFLAMMATION, Neurodegeneration: experimental models < NEURODEGENERATION: CELLULAR AND MOLECULAR, Astrocyte < NEURODEGENERATION: CELLULAR AND MOLECULAR, Microglia < NEURODEGENERATION: CELLULAR AND MOLECULAR, Autoimmune encephalitis < MULTIPLE SCLEROSIS AND NEUROINFLAMMATION, Blood-brain barrier < MULTIPLE SCLEROSIS AND NEUROINFLAMMATION</p>



Behaviour and neuropathology in mice injected with human contactin- associated protein 2 antibodies

Running title: A passive transfer model of CASPR2 antibodies

Maria Pia Giannoccaro^{1,2}, David A. Menassa^{1,3}, Leslie Jacobson¹, Ester Coutinho¹, Gennaro Prota⁴, Bethan Lang¹, M Isabel Leite¹, Vincenzo Cerundolo⁴, Rocco Liguori^{2,5}, Angela Vincent¹

¹ Nuffield Department of Clinical Neurosciences, University of Oxford, Oxford, UK

² Department of Biomedical and Neuromotor Sciences, University of Bologna, Bologna, Italy

³ Biological Sciences, University of Southampton, Southampton, UK

⁴ MRC Human Immunology Unit, Weatherall Institute of Molecular Medicine, John Radcliffe Hospital, University of Oxford, Oxford, UK.

⁵ IRCSS Istituto delle Scienze Neurologiche di Bologna, Bologna, Italy

Correspondence

Prof Angela Vincent, Nuffield Department of Clinical Neurosciences, University of Oxford, Oxford, UK

Email angela.vincent@ndcn.ox.ac.uk

Tel 07817224849

No. Words 5089

No. Pages 22

No. Figures 6

No. Tables 0

Supplementary Material 15 pages, 3 figures

Abstract

Serum antibodies (Abs) that bind to the surface of neurons or glia are associated with a wide range of rare but treatable CNS diseases. In many, if not most instances, the serum levels are higher than CSF levels yet most of the reported attempts to reproduce the human disease in mice have used infusion of Abs into the mouse cerebral ventricle(s) or intrathecal space. We used the intraperitoneal (ip) route and injected purified plasma IgG from either a CASPR2-Ab positive patient (n = ten mice) or healthy individual (n = nine mice) daily for 8 days. Lipopolysaccharide was injected ip on day 3 to cause a temporary breach in the blood brain barrier. A wide range of baseline behaviours, including tests of locomotion, coordination, memory, anxiety and social interactions, were established before the injections and tested from day 5 until day 11. At termination, brain tissue was analysed for human IgG, CASPR2 and c-fos expression, lymphocyte infiltration, and neuronal, astrocytic and microglial markers. Mice exposed to CASPR2-IgG, compared with control-IgG injected mice, displayed reduced working memory during the continuous spontaneous alternation test with trends towards reduced short-term and long-term memories. In the open field tests, activities were not different from controls, but in the reciprocal social interaction test, CASPR2-IgG injected mice showed longer latency to start interacting, associated with more freezing behaviour and reduced non-social activities of rearing and grooming. At termination, neuropathology showed more IgG deposited in the brains of CASPR2-IgG injected mice, but a trend towards increased CASPR2 expression; these results were mirrored in short-term in vitro experiments where CASPR2-IgG binding to hippocampal neurons and to CASPR2-transfected HEK cells led to some internalisation of the IgG, but with a trend towards higher surface expression. Despite these limited results, in the mouse brains there was increased c-fos expression in the piriform-entorhinal cortex and hypothalamus, and a modest loss of Purkinje cells. In the CASPR2-IgG injected mice, there was also increased microglia density, morphological changes in both microglia and astrocytes and raised complement C3 expression on astrocytes, all consistent with glial activation. Patients with CASPR2- Abs can present with a range of clinical features reflecting central, autonomic and peripheral dysfunction. Although the behavioural changes in mice were limited to social interactions and mild working-memory defects, the neuropathological features indicate potentially widespread effects of the antibodies on different brain regions.

Keywords (5): CASPR2 antibodies, animal model, passive transfer, microglia activation, astrocytes

Abbreviations: Ab, antibodies; AR, accelerating rotarod; BBB, blood-brain barrier; CASPR2, Contactin-associated protein 2; CCL5, Chemokine (C-C motif) ligand 5; CD68, cluster of differentiation 68; CSA, continuous spontaneous alternation; DAPI, 4',6-diamidin-2-fenilindolo; DRG, dorsal root ganglia; ECL, enhanced chemiluminescence; eGFP, enhanced green fluorescent protein; FA, forced alternation; GCSF, granulocyte-colony stimulating factor; GFAP, glial fibrillary acidic protein; GM-CSF, granulocyte-macrophage colony-stimulating factor; HC, healthy control; HRP, horseradish peroxidase; IBA1, ionized calcium-binding adapter molecule 1; ICV, intracerebroventricular; IFN- γ , interferon gamma; IgG, immunoglobulin G; IL, interleukin; Ip, intraperitoneally; IS, inverted screen; LDb, light-dark box; LPS, lipopolysaccharide; MB, marble burying test; MCP-1, monocyte chemoattractant protein-1; MCP-5, monocyte chemoattractant protein-5; NA, novel arm; NB, narrow beam; NeuN, neuronal nuclei; NO, novel object/odor; NOR, novel object recognition test; NORf, novel object recognition familiarization phase; NORt, novel object recognition test phase; OF, open field; OT, olfaction test; PBS, perfused with phosphate-buffered saline; PC, Purkinje cells; PFA, paraformaldehyde; RSI, reciprocal social interaction tests; SDS, sodium dodecyl sulphate; SCF, stem cell factor; sTNFRI, Soluble tumor necrosis factor receptor I; TNF α , tumor necrosis factor alpha; TPO, thrombopoietin; TRIS- HCL, tris(hydroxymethyl)aminomethane hydrochloride; VEGF, vascular endothelial growth factor.

Introduction

Antibodies directed against contactin-2 associated protein 2 (CASPR2-Abs) have been associated with a wide range of peripheral (neuromyotonia, pain and autonomic dysfunction) and central nervous system (CNS, cognitive impairment, memory loss, insomnia, hallucinations, delusions, ataxia and epilepsy) symptoms (Irani et al., 2010). In addition, CASPR2-Abs were found in archived gestational sera from mothers whose offspring had neurodevelopmental disorders (Coutinho et al., 2017a); this situation was modelled in a maternal to-fetal transfer study that showed autistic-like behaviour and neuropathological alterations in the offspring of dams injected with CASPR2-Abs (Coutinho et al., 2017b). The effects of several antibodies, most notably those against the NMDA receptor, have been modelled by intraventricular injection (eg. Planagumà et al., 2015; Wright et al., 2015) but there have been no reports of the pathogenicity of CASPR2-Abs in the CNS of adult mice.

CASPR2-Abs are typically at higher titres in serum than in CSF (Sonderen et al., 2016; Bien et al., 2017). Intraperitoneal (ip) injection of purified immunoglobulin G (IgG) from two CASPR2-Abs positive patients to mice over 18 days reduced the thresholds for mechanical stimuli and enhanced the excitability of dorsal root ganglia (DRG) neurons through reductions in Kv1 potassium channel expression but, in that study, brain pathology was not investigated in detail (Fig S3 in Dawes et al., 2018). To explore the effects of CASPR2-Abs in the CNS, we used a similar protocol with 8 daily injections of IgG purified from one patient with autoimmune encephalitis and from one healthy control. We added a single dose of lipopolysaccharide (LPS) at day 3 to disrupt the blood-brain barrier (BBB). We evaluated the effects of the antibodies on mouse behaviours from day 5 of the injections and for 3 days following the last one, and subsequently examined brain pathology. Although previous studies have used a peripheral approach to study antibodies to synaptic vesicle proteins (eg. Amphiphysin, Sommer C et al., 2005; GAD, Chang et al., 2013) this is the first transfer of antibodies to a cell-surface neuronal antigen.

Material and methods

Purification of human IgG

Immunoglobulin G were purified using Protein G Sepharose beads (Sigma, P3296) from a plasma exchange sample of a 71-year old male patient with CASPR2-related encephalitis (CASPR2-IgG) and from sera of one healthy age- and sex-matched individual (HC-IgG) as previously described

(Dawes et al., 2018). The subclasses of the CASPR2-IgG antibodies were determined on the purified IgG (see Supplementary material).

Experimental design and behavioural testing

Animals

The nineteen C57Bl6 male mice aged 6 weeks (18-22 g) were from a licensed breeding establishment (Charles River). The animals were housed in groups of four or five under standard laboratory conditions (ad libitum access to food and water; 12:12 light:dark cycle, with lights on at 7:00) and monitored daily during the experimental period. Mice were tagged and randomly assigned to each experimental group. All in vivo experiments were performed in the Biomedical Services Unit at the John Radcliffe Hospital in accordance with the United Kingdom Home Office Animals in Scientific Procedures Act (1986) and with institutional guidelines. All in vivo and in vitro experiments were performed with animals or tissue coded.

The experimental design is summarised in Fig. 1A. Mice were injected intraperitoneally (ip) daily with either CASPR2-IgG (ten mice, 20 mg/ml Day 0 (D0) and 12 mg until D8) or HC-IgG (nine mice, 20 mg/ml D0, 12 mg D1-2 and 6 mg/ml until D8). At day 3 all animals were injected ip with LPS (1 mg/Kg from E. Coli O111.B4, L3012, Sigma Aldrich, UK). At day 11 animals were sacrificed.

Behavioural tasks were performed according to standardized tests (eg. Coutinho et al., 2017b) blind to the animal status and following the schedule summarized in Fig. 1A. All tests, with the exception of the reciprocal social interaction and the olfactory tests, were performed for up to 5 days before D0 and from D5 till D11 during and after the IgG injections. A description of each task is provided in the Supplementary Material.

Blood and brain tissue processing

At day 11, eleven animals (6 CASPR2-IgG and 5 HC-IgG injected) were randomly selected and sacrificed by CO₂. Blood samples were collected by cardiac puncture, centrifuged and the sera were stored at -20°C before testing by cell-based assay for CASPR2-IgG (see Supplementary Material). Brains were harvested and snap-frozen for protein extraction. The remaining eight animals (4/group) were perfused with phosphate-buffered saline (PBS) followed by ice-cold 4% paraformaldehyde (PFA). Brains were removed, post-fixed, cryoprotected with 30% sucrose in PBS and snap-frozen. All brains were stored at -80 °C.

Morphological and immunofluorescence analysis of the brain

Neuropathological studies were performed as previously described (Coutinho et al., 2017b) and are detailed in Supplementary Material. PFA-perfused fixed brain sections were cut at 50 μm thickness using a Leica CM1900 cryostat. Confocal images were taken of immunofluorescently labeled brain sections using a Zeiss LSM 710 confocal microscope and images were analysed with FiJi software (Open Source HR Software). Brightfield images were taken using the Aperio ScanScope (Leica Biosystem) and analysed in ImageScope (Leica Biosystem). To evaluate gross morphology, sections were Nissl-stained with Cresyl Violet (C5042, Sigma Aldrich, UK).

To look at the similarity between CASPR2 and IgG staining, two consecutive series were incubated with anti-human IgG antibodies (Biotium, 20022, 1:500) and with rabbit monoclonal anti-CASPR2 antibodies (Abcam, UK, Ab137052, 1:500) respectively.

Neurons and astrocytes were identified by immunofluorescence using anti-NeuN (Merck, MAB377, 1:500) and anti-glial fibrillary acidic protein (GFAP) (Dako, 203334, 1:500) respectively. For neuronal c-fos, sections were co-stained with anti-c-fos (Abcam, ab190289, 1:100) and anti-NeuN antibodies. In the cerebellum, anti-calbindin D28K antibody (Millipore, AB1778; 1:200) was used for the identification of Purkinje cells (PC). Astrocyte morphology was assessed in GFAP expressing cells and also by co-staining for complement C3 (Abcam, Ab200999, 1:100).

Microglial density was measured with anti-IBA1 (Wako chemicals, 019-19741, 1:500) and anti-CD68 (BioRad, MCA1957; 1:400) markers. Soma size (μm^2), total cell body size (μm^2) and the soma/total cell body size ratio was used to assess microglial activation, as previously described (Coutinho et al., 2017). Cellular infiltration of B and T lymphocytes was assessed using the CD19 (Abcam, 1:100, ab25232) and the CD3 (Abcam, 1:100, ab16669) antibody markers, respectively.

Immunoblot analysis

Whole brains (3 per group) were homogenised in lysis buffer (50 mM TRIS-HCL, 150 mM NaCl, 0.1% SDS, 1% triton-X 100, pH 7.4) supplemented with protease inhibitors (1:100) and applied to SDS-polyacrylamide gels, transferred to nitrocellulose membranes and probed with rabbit anti-CASPR2 (Abcam, ab137052, 1:1000) and anti-GAPDH antibodies (Abcam, ab181602, 1:2000) followed by HRP-coupled secondary antibody. Antibody binding was detected by enhanced chemiluminescence (ECL) (Amersham GE Healthcare) and captured on autoradiography film (GE Healthcare). Films were scanned and signals quantified using Fiji ImageJ software. Each brain

extract was tested four times and the mean intensities of signal for CASPR2-IgG mice was compared with the mean intensities of HC-IgG mice.

Brain cytokine expression was analyzed using a Mouse Cytokine Antibody Array (22 Targets) (Abcam, 133993) as per the manufacturer's instructions. Immunoreactivity was then visualized using ECL and analysed using Fiji as above. Positive controls were included on each membrane and used for normalisation. Because of the range of different values for each test substance, the CASPR2-IgG intensities were expressed relative to the signal for the HC-IgG intensities (as in Dawes et al., 2018).

In vitro experiments

To look in more detail at the effects of CASPR2-Abs, hippocampal neurons and CASPR2-transfected HEK cells were exposed to CASPR2-IgG and HC-IgG for between 30 mins to 24 hours at 37 C. The binding of IgG to the surface of unpermeabilised cells, and presence of IgG intracellularly in fixed permeabilised cells, was measured by confocal microscopy and flow cytometry (FACS). FACS was used to measure CASPR2 expression using an extracellular (Abcam, UK, 105581) and an intracellular (Abcam, UK, ab33994) anti-CASPR2 commercial antibody (both 1:200). Details of the methods are given in Supplementary material.

Statistics

A student's t-test or a Mann-Whitney were used for comparison between groups as appropriate. Holm-Sidak was applied to correct for multiple comparisons. Behavioural data were analysed by one-way ANCOVA, using the baseline as a covariate, or with two-way mixed ANOVA. Transformations were applied if necessary to meet normality or to adjust for inequality of variances. Repeated measure ANOVA or two-way mixed ANOVA was performed on flow cytometry data. Significance was placed at $P < 0.05$. Statistical tests were carried with IBM SPSS statistics version 20.0 (SPSS Inc., Chicago, USA). Data in the text are presented as mean \pm SDs, CASPR2-IgG vs HC-IgG mice. Graphs are plotted as mean \pm SEMs (Graph Pad prism version 6, GraphPad software, San Diego, California, USA).

Results

CASPR2-IgG injected mice have mild cognitive and behavioural impairments

Exposure to most of the behavioural tests was performed during the 5 days preceding the start of the injections; testing was then conducted during the injections (D5-7) and for the 3 days following the final injection (D8- 10) (see Fig 1A). A cell-based assay for CASPR2-Abs confirmed high levels in the CASPR2-IgG injected mice even on Day 11, 4 days after the last IgG injection (Fig 1B). Body weights over the period of the experiment, motor tests (accelerating rotor-rod, inverted screen, multiple narrow beams) and tests of anxiety (open field, light-dark box test) at D5-9 showed no differences between the two groups (Supplementary Material Fig. 1). These observations suggested no effect of the CASPR2-Abs on general health or well-being.

There were differences, however, between CASPR2-IgG and HC-IgG injected mice with respect to cognitive and social activities. The following results are given as mean \pm SD, CASPR2-IgG vs HC-IgG unless otherwise stated. The CASPR2-IgG injected mice showed reduced numbers of spontaneous alternations at D10 ($F(1,16) = 4.75$, $P = 0.04$, partial $\eta^2 = 0.22$, two-way mixed ANOVA; 55 ± 10.9 vs 68.8 ± 10.3 (with one outlier removed); Fig. 1C) suggestive of a working memory impairment. This finding was supported by the 50% of CASPR2-IgG injected mice that showed same arm re-entries compared with 11% of HC-IgG injected. CASPR2-IgG injected mice also showed trends towards a reduced preference index for entries in the new arm in the forced alternation task at Day 8 ($F(1,16) = 3.36$, $P = 0.085$; 0.07 ± 0.46 vs 0.33 ± 0.3 ; Fig. 1D), and reduced preference index ($F(1,16) = 2.45$, $P = 0.14$; 0.06 ± 0.32 vs 0.26 ± 0.25 ; Fig. 1E) in the novel object recognition test on D10.

Social and non-social behaviours were tested by the reciprocal social interaction test on D10. CASPR2-IgG injected mice showed longer latency to start interacting compared to HC-IgG injected mice ($U = 5.5$, $P = 0.04$; Mann-Whitney test U, Fig. 1F; 41.9 ± 78 vs 13.4 ± 21.2) but similar interaction time and number of interactions. In non-social activities (Fig. 1G), including grooming and locomotor activity, CASPR2-IgG injected animals showed less exploratory behaviour with longer time spent immobile ($t(22) = 3.42$, $P = 0.002$; t-test; 98.6 ± 43.2 vs 46.6 ± 30.1) and reduced rearing ($t(22) = 3.01$, $P = 0.006$; t-test; 13 ± 8.8 vs 26 ± 12) compared to HC-IgG injected animals. In addition, the CASPR2-IgG injected group had reduced grooming events ($t(22) = 2.61$, $P = 0.015$; t test; 2.6 ± 1 vs 3.8 ± 1.1), but a longer duration of each self-grooming bout ($t(22) = 2.48$, $P = 0.002$; t test; 2.9 ± 1.1 vs 2 ± 0.6). Equivalent non-social behaviors had been assessed during the open field and no differences were observed between groups (Supplementary Material Fig. 1), suggesting that the changes shown in Figure 1G reflected an influence of the social context. Importantly, olfactory function, which can influence social activities, was similar in the two groups on D9 (Fig. 1H).

CASPR2-IgG accesses the brain but does not alter CASPR2 expression

The distribution of human IgG was investigated in different brain regions by immunofluorescence (Fig. 2A). The level of deposited IgG was higher in the cortex ($t(6)=2.71$, $P=0.03$, t-test; mean fluorescence intensity (MFI): 130.9 ± 31.6 vs 85.3 ± 11.1), hippocampus ($t(6)=3.03$, $P=0.023$, t-test; 92.2 ± 12.4 vs 68.8 ± 9.1), and thalamus ($t(6)=7.14$, $P=0.0004$, t-test; 137.3 ± 20 vs 61 ± 7.3) of CASPR2- IgG injected mice compared to controls (Fig. 2A,B). Nevertheless, there were no apparent differences in CASPR2 expression, measured by a commercial anti-CASPR2 antibody, between the two groups in these areas (Fig. 2A and 2C), or when total CASPR2 protein was quantified by western blot (WB) in whole brain lysates, where there was a trend towards increased CASPR2 expression ($t(6)=1.7$, $P=0.13$; optical density (OD): 1.9 ± 0.2 vs 1.5 ± 0.2 ; Fig. 2D).

Effects of CASPR2-IgG antibodies in vitro

Although the absence of CASPR2 loss mirrored previous in vitro findings (Patterson et al., 2018), the effects of CASPR2-IgG were further explored in vitro. First, we measured the subclasses of the CASPR2 antibodies as these are relevant to the potential mechanisms. Although mostly IgG4 (72%), there was also IgG1 (22%) and a little IgG2 (6%); IgG3 was <1% of the total. We then looked at the effects on rat hippocampal cultured neurons. After 24 h incubation with CASPR2-IgG, an increase in intracellular IgG ($t(28)=7.02$, $P < 0.0001$, unpaired t test with Welch's correction; puncta density T 30 min vs T 24h: 0.46 ± 0.17 vs 7.66 ± 1 total 71 segments examined from 2 experiments) was observed without a reduction of the density of extracellular puncta (Fig 2E), suggesting some internalisation of the IgG. To pursue further we studied CASPR2 IgG or HC IgG binding to CASPR2-transfected HEK cells and IgG internalisation by confocal imaging. After 24 h incubation, live cells were stained with anti-human IgG 568 (red) secondary antibodies, then fixed, permeabilised and stained again with anti-human IgG 488 (green) secondary antibodies. There was no apparent loss of surface IgG binding but evidence of cytoplasmic IgG aggregates; this was demonstrated graphically by profile plots of mean fluorescence intensity across the cells that showed the presence of cytoplasmic IgG after 24 h incubation with CASPR2-IgG without, however, significant changes in the membrane IgG binding (Fig 3A). These results were confirmed by analysis of the fluorescence intensity of the IgG on the membrane and in the cytoplasm: membrane IgG was unchanged over time whereas intracellular IgG was increased at 24 h compared to 30 min ($t(55)=3.10$, $P=0.003$, unpaired t test with Welch's correction; MFI at 30m vs 24h: 35.08 ± 2.3 vs 54.95 ± 5.9 , $N=102$ cells from 2 experiments).

To confirm these findings, we repeated the experiment using flow cytometry (FACS). In this case we also used two additional CASPR2-Abs patients and one more control. Examples are shown in Figure 3B and results summarised in Fig 3C. Although not significant, there was an increase in extracellular IgG binding as shown by an increase in the percentage of double-stained cells (Fig 3B upper right quadrant) and MFI values ($F(1.6, 3.3)=5.4$, $P=0.09$, repeated measure ANOVA with Greenhouse-Geisser correction; Fig. 3C, top) over the first few hours, that plateaued by 6-16 hours. Intracellular IgG was found in a variable proportion of the CASPR2-IgG bound cells between the three patients ($F(1.09, 2.31)=1.4$, $P=0.35$, repeated measure ANOVA with Greenhouse-Geisser correction), roughly correlating with IgG bound extracellularly (Fig 3C, bottom). We also looked in parallel at CASPR2 expression using an extracellular CASPR2 antibody and an intracellular CASPR2 antibody (Fig 3D). The extracellular antibody showed a trend towards increased levels over the first 16 hours in CASPR2-IgG compared with HC-IgG treated cells ($F(1,4)=3.1$, $P=0.14$, two-way mixed ANOVA) (Fig 3E, top); thereafter, extracellular CASPR2 expression declined in both CASPR2 and HC-IgG treated cells. By contrast, there was no difference between CASPR2 expression using the intracellular CASPR2 antibody between HC-IgG and CASPR2-IgG patients at any time point ($F(1,4)=0.16$, $P=0.7$, two-way mixed ANOVA) (Fig 3E bottom).

CASPR2-IgG exposure does not cause generalised neuronal loss

No gross morphological changes were observed on Nissl-stained sections between the two groups for hippocampal, cerebellar and total brain volume. The thickness of the cortical (anterior cingulate, primary motor, somatosensory, piriform cortices), hippocampal and cerebellar layers was also not different (Supplementary Material Fig 2).

Densities of NeuN-positive neurons were measured in the somatosensory, piriform cortex, hippocampus and cerebellum. No evidence of neuronal loss was found in the CASPR2-IgG compared to the HC-IgG injected mice in the cortical areas or in the hippocampus (Fig. 4A, B). In the cerebellum, however, despite no difference in the count of NeuN positive cells in the molecular layer, there was a 14.6% reduction in the number of calbindin-positive Purkinje cells ($t(6)=2.45$, $P=0.049$, t-test: 34.3 ± 3.4 vs 40.2 ± 3.3) (Fig. 4C).

C-fos expression is a marker of neuronal activity and was measured on NeuN stained neurons. Compared to the HC-injected mice, mice injected with CASPR2-IgG showed a higher density of c-fos expressing neurons in the entorhinal-piriform cortex ($t(6)=3.11$, $P=0.020$, t-test; 6574 ± 1694 vs 3167 ± 1389), dorsomedial ($t(6)=2.67$, $P=0.036$; t test; 6743 ± 1090 vs 4304 ± 1462) and lateral

($t(6)=2.79$, $P=0.031$, t test; 11238 ± 4313 vs 4955 ± 1277) hypothalamus (Fig. 4D). No differences between groups in the density of c-fos expressing neurons were detected in the hippocampus, somatosensory cortex and amygdala.

CASPR2-IgG injected mice display microglial activation and increased microglia density

Activated microglial cells, as identified by expression of IBA1 and CD68 (Fig. 5A), were measured in the somatosensory and piriform cortices, the hippocampus and the cerebellum. Microglial density was increased in the somatosensory cortex of CASPR2-IgG injected mice ($t(6)=2.63$, $P=0.038$, t test; 12169 ± 355 vs 10550 ± 1177) and molecular layer of the cerebellum ($t(6)=4.99$, $P=0.002$, t test; 3432 ± 378.5 vs 2481 ± 35.2) but not in the piriform cortex, the hippocampus or the granular layer of the cerebellum (Fig. 5B).

Analysis of microglial morphology was performed on IBA1 positive cells (Fig. 5C) in the hippocampus and in the molecular layers of the cerebellum. When activated, microglia assume an ameboid morphology characterized by a larger soma body and shorter processes. In the hippocampus, microglia from CASPR2-IgG injected mice showed a higher cell soma/cell total body size ratio ($t(6)=4.74$, $P=0.0032$, t -test; 0.092 ± 0.005 vs 0.068 ± 0.008), less ($t(6)=3.27$, $P=0.017$, t -test; 4 ± 0.1 vs 4.28 ± 0.1) and shorter ($t(6)=3.68$, $P=0.010$, t -test; 29.04 ± 0.9 vs 35.07 ± 3.1) ramifications than HC-IgG injected mice, compatible with an activated phenotype. Similar results were found in the molecular layer of the cerebellum, with a higher soma/total body area size ratio ($t(6)=7.35$, $P=0.0003$, t -test; 0.051 ± 0.004 vs 0.029 ± 0.003) and shorter ramification maximal length ($t(6)=3.68$, $P=0.008$, t -test; 39.08 ± 4.8 vs 48.87 ± 1.4) than HC-IgG exposed mice (Fig. 5D); no significant difference was seen in the number of ramifications.

CASPR2-IgG injected mice display astrocytic activation without overt astrocytosis

There were no differences in the density of GFAP-positive cells in the somatosensory and piriform cortices, or in the hippocampus (data not shown) but increased GFAP expression in the molecular layer of the cerebellum ($t(6)=2.55$, $P=0.043$, t -test; MFI 106.7 ± 12.5 vs 83.97 ± 12.7) (Fig. 6A). Nevertheless, there was evidence of reactive astrocytosis as indicated by complement C3 and GFAP co-expression. The C3/GFAP co-stained area was raised in CASPR2-IgG injected mice in the hippocampus ($t(398)=4.87$, $P<0.0001$, 200/cells per group, t -test; 60.69 ± 32.6 vs 47.88 ± 17.8), somatosensory cortex ($t(160)=2.41$, $P=0.01$, 81/cells per group, t -test; 55.53 ± 24.2 vs $47.07 \pm$

20.09) and cerebellum ($t(204)=7.14$, $P < 0.0001$, 103/cells per group, t-test; 78.99 ± 16.8 vs 61.19 ± 18.8) (Fig. 6B). The astrocytes from CASPR2-IgG injected mice also showed a smaller cell total body size ($U=22052$, $P= 0.0051$, 228/cells per group Mann Whitney test U; median CASPR2- vs HC-IgG: 366.9 vs 397.8) and shorter ($U=19946$, $P < 0.0001$, Mann Whitney test U; median CASPR2- vs HC-IgG: 18.67 vs 21.06) maximal ramification length than HC- IgG injected mice, compatible with an activated phenotype, in the hippocampus (Fig. 6C).

As these microglial and astrocyte changes suggested a state of mild neuroinflammation in the CASPR2-IgG injected mice, we assessed the presence of B and T cells infiltrates. CD19- and CD3- positive cells were sparse and observed mainly in the meninges and choroid plexus, and only very rarely in the parenchyma (Supplementary Figure 3). Additionally, a commercial cytokine/chemokine array was performed on three whole brain lysates from each group to look for changed neuroinflammatory markers. A trend towards increased levels was noted for several cytokines and chemokines, and particularly for interleukin (IL)-10, stem cell factor (SCF), and vascular endothelial growth factor (VEGF), but none reached significance after correction for multiple comparisons (Fig. 6D).

Discussion

Many of the recently-described antibody-mediated CNS diseases have higher serum antibodies than CSF antibody levels, emphasizing that in many or most cases they are likely to be initiated by a peripheral immune response. It was timely, therefore, to see whether peripheral injection of antibodies could, under conditions where the blood brain barrier is briefly compromised, lead to evidence of CNS dysfunction. CASPR2-Ab at very high serum titers have been identified in patients with both peripheral and central neurological disorders. Here we showed that, after intraperitoneal (ip) injection of CASPR2-IgG with one dose of lipopolysaccharide, the antibodies reached the mouse brain parenchyma, and were associated with mild changes in cognitive and in socially-dependent non-social behaviours; the mouse brains showed increased activated microglia and astrocytes and increased c-fos expression, but no evidence of neuronal loss or reduction in CASPR2 expression.

Previous studies showed that LPS is able to breach the BBB (Kowal et al., 2004; Banks et al., 2015) and allow peripherally administered antibodies to penetrate the brain parenchyma without causing, *per se*, sustained neurotoxicity or neuroinflammation (Kowal et al., 2004). We used a single injection of LPS during a peripheral passive transfer of IgG into adult mice, similar to that used in many previous studies on peripheral disorders (Fukunaga et al., 1983; Piddlesden et al., 1996;

Viegas et al., 2012), and recently sensory hypersensitivity (Dawes et al., 2018). Human IgG was present in the brain of both control and CASPR2-IgG injected mice, as would be expected after LPS but, in all areas except the cerebellum, the intensity was higher in the CASPR2-IgG injected mice.

Most antibody-mediated diseases act, at least partially, by antigenic modulation by which the antibodies cross-link and internalise their target, but we found no reduction of CASPR2 expression on immunohistology. A recent study in vitro found that CASPR2-Abs did not reduce CASPR2 expression on the surface of cultured hippocampal neurons, but that they inhibited the interaction of CASPR2 with its extracellular binding partner, contactin2 (Patterson et al., 2018). In vivo, CASPR2-Abs reduced the surface expression of Kv1 on DRG neurons (Dawes et al., 2018) but specific mechanism was not studied. In the current model, we cannot exclude that by the time the neuropathology was performed, on day 11, compensatory mechanisms may have occurred to restore CASPR2 expression. Indeed, a trend towards higher levels of CASPR2 levels was seen in the brain extracts of CASPR2-IgG injected mice, and our in vitro neuronal and HEK experiments, also showed a trend towards higher levels of CASPR2 surface expression after 6-16 hours exposure to CASPR2 antibodies, as well as some IgG internalisation, which was not investigated in the previous study (Patterson et al., 2018). Thus it appears that some CASPR2-IgG is internalised, which would be expected because of the presence of IgG1 divalent antibodies in the CASPR2-IgG preparation; but apparently this was not sufficient to cause loss of CASPR2 from the cell surface and the trend towards higher CASPR2 expression, both in vivo and in vitro, suggests that there might be some compensatory changes.

Behaviourally, during the social interaction test CASPR2-IgG injected mice showed longer latency to interact but otherwise normal sociability. However, they showed increased immobility and anxiety-like behaviour and, since the same non-social activities were normal during other tests (i.e. open field), these behaviours are likely to be related to the social novelty context (Meeker et al., 2013). This interpretation is also supported by the longer grooming bout during the same test (Kalueff and Tuohimaa, 2004). These observations need to be explored in more detail in the future.

CASPR2-IgG injected mice showed less alternation in the continuous spontaneous alternation tests, with similar trends in the forced alternation and novel object recognition tests. These findings might seem inconsistent with the lack of histological changes in the hippocampus. However, although working memory is related to hippocampal integrity, other brain areas play a role in these tasks (Lalonde, 2002). Among those, the entorhinal cortex, where CASPR2 is highly expressed (Gordon et al., 2016), is the main source of hippocampal afferents from the neocortex and is involved in

different forms of memory (van Groen et al., 2003). Indeed, in mouse models of Alzheimer's disease, memory impairment was associated with an early hyper-excitability of the entorhinal cortex (Xu et al., 2015) which would be consistent with increased neuronal excitability following reduction in Kv1 expression which was seen in the dorsal root ganglia in the peripheral CASPR2-Ab model (Dawes et al., 2018).

These changes may also have been responsible for the higher levels of c-fos expression in the entorhinal-piriform cortex, rather than in the hippocampus. Interestingly, increased c-fos expression was also observed in the dorsomedial and lateral hypothalamus. The lateral hypothalamus is related to the sleep-wake cycle, with increased levels of c-fos expression during the dark period, when the mice are active (Basheer et al., 1997). Thus, an increase of c-fos expression during the light period in our animals might suggest an increased wakefulness, consistent with the insomnia typically observed in patients with Morvan's Syndrome (Liguori et al., 2001). Clearly, further experimental studies on the effects of CASPR2-Ab on sleep are also needed.

Consistently with previous findings (Dawes et al., 2018), CASPR2-Ab did not cause evident neuronal loss, except in the cerebellum, where there was a mild loss of Purkinje cells. CASPR2-Abs bind to the axons of granule cerebellar neurons in the molecular layer and have been associated with cerebellar ataxia in some patients (Becker et al., 2012), as well as with morphological changes of Purkinje cells in a neuropathological case (Sundal et al., 2017). The only 14.6% loss of these cells might explain why we did not observe coordination difficulties in the mice in the accelerating rotarod or narrow beam.

One striking finding was the activation of microglia and astrocytes. Microglia and astrocytes are responsible for the innate immunity in the brain and their functions are strictly interconnected. Previous studies showed that in pathological conditions (Lian et al., 2016; Liddelow et al., 2017), activated microglia were able to induce reactive astrocytes, which up-regulate C3 expression and become responsible for neurotoxicity and loss of synapses. Accordingly, alongside microglia activation and increased density, we found increased C3 expression on the surface of astrocytes and higher numbers of activated astrocytes in CASPR2-IgG injected mice. The microglial and astrocytic activation was particularly evident in the cerebellum where reactive microglia have been associated with PC loss in a mouse model of cerebellar degeneration (Zhao et al., 2011). Finally, although there were no significant changes in cytokine or chemokine expression when examined at termination, even after correction for multiple comparisons there were trends towards increased levels of those relevant to glial activity. The lack of an overt inflammatory response was further

supported by the absence of B and T cells infiltrates in the brain parenchyma, in accordance with previous findings in the spinal cord (Dawes et al., 2018).

Microglial activation has been reported in neuropathological cases of patients with CASPR2-Ab encephalitis (Körtvelyessy et al., 2015; Sundal et al., 2017). Moreover, microglial activation and increased density was noted in cortex of animals exposed to CASPR2-Abs in utero and this activation persisted into adulthood (Coutinho et al., 2017b). By contrast, the peripheral administration of CASPR2-IgG, without LPS, induced only a mild increase of microglia in the spinal cord but not in the somatosensory cortex of exposed animals (Dawes et al., 2018), suggesting that the microglial activation in this model is dependent on the effects of CASPR2-IgG in the brain.

Our study has several limitations. First, we used whole IgG rather than cloned CASPR2-IgG antibodies. The purified IgG did not bind to CASR2-null mouse brain tissue (Coutinho et al., 2017b) and the results of transfer from mother to offspring of the IgG were similar to those obtained with a monoclonal CASPR2 antibody (Brimberg et al., 2017). It was concluded that the effects seen were largely or only due to the CASPR2 specific antibodies. Second, only one case and one control were studied and unfortunately the yield of control serum IgG was limited and not sufficient to match the CASPR2-IgG over the full course of the injections, although the amounts were matched until the LPS injection. Third, the experimental timing we chose could mean that we missed the acute effects of the antibodies while some behavioural and histological effects might have required more time to become fully established. Fourth, the use of LPS, could have induced additional inflammation and contributed to determining the site of BBB disruption, leading to, or changing, some of the antibody effects we observed. However, previous studies in our laboratory and elsewhere have shown that IgG penetration into the brain in the absence of LPS is low (Braniste et al., 2014) and that LPS is necessary to produce an effective transfer to the brain parenchyma (Kowal et al., 2004). Moreover, in a similar transfer experiment with glutamic-acid decarboxylase antibodies and two doses of LPS (Chang et al 2012), any human IgG bound was restricted to hippocampus and brain stem areas, compared to the wider distribution seen here for CASPR2-IgG antibodies. The alternative approach of intracerebroventricular (ICV) injection of the antibodies would have overcome the need to use LPS to open the BBB, but there is no evidence yet that the ICV approach provides a more complete model of autoimmune disorders such as NMDAR-Ab encephalitis (Planagumà et al., 2015; Wright et al., 2015), since in neither case were there movement disorders or spontaneous seizures seen in the NMDAR-Ab infused mice. Nevertheless, as there little understanding about the relative roles of CSF and serum antibodies in some of these conditions, a direct comparison between the peripheral and intraventricular approaches could be

very interesting. Finally, many questions remain unanswered such as the full mechanisms by which CASPR2-Abs affect brain, whether the glial changes are relevant to the human disease, and if they are dependent on the specificity of the antibody or common to all forms of autoimmune encephalitis.

Despite the limitations, our findings demonstrate that peripherally administered CASPR2-Abs, in the presence of a temporary breach in the BBB, are able to access the brain and produce histological and behavioural changes. These data support a pathogenic role of CASPR2-IgG in mediating the CNS symptoms observed in patients with encephalitis and lead the way for more detailed studies on how and where the antibodies act to cause the full range of clinical features.

Acknowledgements

We are very grateful to Prof D Bannerman for his advice regarding behavioural testing, and to Prof David Bennett, Drs Steven West and John Dawes for advice regarding the confocal measurements.

Funding

There was no specific funding for this study. MPG was supported by the Department of Biomedical and Neuromotor Sciences, University of Bologna. EC was funded by the Programme for Advanced Medical Education, Fundação Calouste Gulbenkian. We are very grateful to the Nuffield Department of Clinical Neurosciences for their contributions to the further support of the project (MPG, LJ, DM, BL).

Conflict of interest

The University of Oxford holds patents for LGI1, CASPR2 and Contactin2 antibodies, licensed to Euroimmun AG for antibody assays. AV and BL receive a proportion of royalties.

References

Banks WA, Gray AM, Erickson MA, Salameh TS, Damodarasamy M, Sheibani N, et al. Lipopolysaccharide-induced blood-brain barrier disruption: Roles of cyclooxygenase, oxidative stress, neuroinflammation, and elements of the neurovascular unit. *J. Neuroinflammation* 2015; 12: 1–15.

- Basheer R, Sherin JE, Saper CB, Morgan JI, McCarley RW, Shiromani PJ. Effects of sleep on wake- induced c-fos expression. *J. Neurosci.* 1997; 17: 9746–9750.
- Becker EBE, Zuliani L, Pettingill R, Lang B, Waters P, Dulneva A, et al. Contactin-associated protein-2 antibodies in non-paraneoplastic cerebellar ataxia. *J. Neurol. Neurosurg. Psychiatry* 2012; 83: 437–440.
- Bien CG, Mirzadjanova Z, Baumgartner C, Onugoren MD, Grunwald T, Holtkamp M, et al. Anti-contactin-associated protein-2 encephalitis: relevance of antibody titres, presentation and outcome. *Eur. J. Neurol.* 2017; 24: 175–186.
- Braniste V, Al-Asmakh M, Kowal C, Anuar F, Abbaspour A, Tóth M, et al. The gut microbiota influences blood-brain barrier permeability in mice. *Sci Transl Med.* 2014; 6:263ra158.
- Brimberg L, Mader S, Jeganathan V, Berlin R, Coleman TR, Gregersen PK, et al. Caspr2-reactive antibody cloned from a mother of an ASD child mediates an ASD-like phenotype in mice. *Mol Psychiatry.* 2016; 21: 1663-1671.
- Chang T, Alexopoulos H, McMenamin M, Carvajal-González A, Alexander SK, Deacon R, et al. Neuronal surface and glutamic acid decarboxylase autoantibodies in Nonparaneoplastic stiff person syndrome. *JAMA Neurol.* 2013; 70: 1140-9.
- Coutinho E, Jacobson L, Pedersen MG, Benros ME, Nørgaard-Pedersen B, Mortensen PB, et al. CASPR2 autoantibodies are raised during pregnancy in mothers of children with mental retardation and disorders of psychological development but not autism. *J Neurol Neurosurg Psychiatry.* 2017a; 88: 718-721.
- Coutinho E, Menassa DA, Jacobson L, West SJ, Domingos J, Moloney TC, et al. Persistent microglial activation and synaptic loss with behavioral abnormalities in mouse offspring exposed to CASPR2-antibodies in utero. *Acta Neuropathol.* 2017b; 134: 567–583.
- Dawes JM, Weir GA, Middleton SJ, Patel R, Chisholm KI, Pettingill P, et al. Immune or Genetic-Mediated Disruption of CASPR2 Causes Pain Hypersensitivity Due to Enhanced Primary Afferent Excitability. *Neuron* 2018; 97: 806–822.e10.
- Fukunaga H, Engel AG, Lang, B, Newsom Davis J, Vincent A. Passive transfer of Lambert-Eaton myasthenic syndrome with IgG from man to mouse depletes the presynaptic membrane active zones. 1983; 80: 7636–7640.

Gordon A, Salomon D, Barak N, Pen Y, Tsoory M, Kimchi T, et al. Expression of Cntnap2 (Caspr2) in multiple levels of sensory systems. *Mol. Cell. Neurosci.* 2016; 70: 42–53.

van Groen T, Miettinen P, Kadish I. The entorhinal cortex of the mouse: Organization of the projection to the hippocampal formation. *Hippocampus* 2003; 13: 133–149.

Irani SR, Alexander S, Waters P, Kleopa KA, Pettingill P, Zuliani L, et al. Antibodies to Kv1 potassium channel-complex proteins leucine-rich, glioma inactivated 1 protein and contactin-associated protein-2 in limbic encephalitis, Morvan's syndrome and acquired neuromyotonia. *Brain* 2010; 133: 2734–2748.

Kalueff A V., Tuohimaa P. Grooming analysis algorithm for neurobehavioural stress research. *Brain Res. Protoc.* 2004; 13: 151–158.

Körtvelyessy P, Bauer J, Stoppel CM, Brück W, Gerth I, Vielhaber S, et al. Complement-associated neuronal loss in a patient with CASPR2 antibody-associated encephalitis. *Neurol. Neuroimmunol. NeuroInflammation* 2015; 2: e75.

Kowal C, DeGiorgio L a., Nakaoka T, Hetherington H, Huerta PT, Diamond B, et al. Cognition and Immunity. *Immunity* 2004; 21: 179–188.

Lalonde R. The neurobiological basis of spontaneous alternation. *Neurosci. Biobehav. Rev.* 2002; 26: 91–104.

Lian H, Litvinchuk XA, Chiang AC, Aithmitti N, Jankowsky JL. Astrocyte-Microglia Cross Talk through Complement Activation Modulates Amyloid Pathology in Mouse Models of Alzheimer ' s Disease. 2016; 36: 577–589.

Liddel SA, Guttenplan KA, Clarke LE, Bennett FC, Bohlen CJ, Schirmer L, et al. Neurotoxic reactive astrocytes are induced by activated microglia. *Nature* 2017; 541: 481–487.

Liguori R, Vincent A, Clover L, Avoni P, Plazzi G, et al. Morvan's syndrome: peripheral and central nervous system and cardiac involvement with antibodies to voltage-gated potassium channels. *Brain* 2001; 124: 2417–2426.

Meeker HC, Chadman KK, Heaney AT, Carp RI. Assessment of social interaction and anxiety-like behavior in senescence-accelerated-prone and -resistant mice. *Physiol. Behav.* 2013; 118: 97–102.

Patterson KR, Dalmau J, Lancaster E. Mechanisms of Caspr2 antibodies in autoimmune encephalitis and neuromyotonia. *Ann. Neurol.* 2018; 83: 40–51.

Piddlesden SJ, Jiang S, Levin JL, Vincent A, Morgan BP. Soluble complement receptor 1 (sCR1) protects against experimental autoimmune myasthenia gravis. *J. Neuroimmunol.* 1996; 71: 173–177.

Planagumà J, Leypoldt F, Mannara F, Gutiérrez-Cuesta J, Martín-García E, Aguilar E, et al. Human N-methyl D-aspartate receptor antibodies alter memory and behaviour in mice. *Brain* 2015; 138: 94– 109.

Sommer C, Weishaupt A, Brinkhoff J, Biko L, Wessig C, Gold R, Toyka KV. Paraneoplastic stiff-person syndrome: passive transfer to rats by means of IgG antibodies to amphiphysin. *Lancet.* 2005; 365: 1406-11.

Sonderen A Van, Ariño H, Petit-Pedrol M, Leypoldt F, Körtvélyessy P, Lancaster E, et al. The clinical spectrum of Caspr2 antibody – associated Neurology. 2016; 87: 521-8.

Sundal C, Vedeler C, Miletic H, Andersen O. Morvan syndrome with Caspr2 antibodies. Clinical and autopsy report. *J. Neurol. Sci.* 2017; 372: 453–455.

Viegas S, Jacobson L, Waters P, Cossins J, Jacob S, Leite MI, et al. Passive and active immunization models of MuSK-Ab positive myasthenia: Electrophysiological evidence for pre and postsynaptic defects. *Exp. Neurol.* 2012; 234: 506–512.

Wright S, Hashemi K, Stasiak L, Bartram J, Lang B, Vincent A, et al. Epileptogenic effects of NMDAR antibodies in a passive transfer mouse model. *Brain* 2015; 138: 3159–3167.

Xu W, Fitzgerald S, Nixon RA, Levy E, Wilson DA. Early hyperactivity in lateral entorhinal cortex is associated with elevated levels of A β PP metabolites in the Tg2576 mouse model of Alzheimer's disease. *Exp. Neurol.* 2015; 264: 82–91.

Zhao Z, Wang J, Zhao C, Bi W, Yue Z, Ma ZA. Genetic ablation of PLAG6 in mice leads to cerebellar atrophy characterized by purkinje cell loss and glial cell activation. *PLoS One* 2011; 6

Figure legends

Figure 1. Experimental design and selected behavioural tests. (A) Experimental design. The behavioural tasks assessed locomotion (open field, OF), strength (inverted screen, IS), coordination (accelerating rotarod, AR and narrow beam, NB), working memory (continuous spontaneous alternation, CSA), short- (forced alternation, FA) and long-term memory (novel object recognition, NOR - NORf, familiarization phase, NORf test phase), anxiety (light-dark box, LDb), compulsive-like behaviour (marble burying test, MB), social behavior (reciprocal social interaction tests, RSI) and olfaction (olfaction test, OT). (B) Representative images of cell-based assays showing CASPR2- Ab in the serum from a CASPR2-IgG injected mouse but not in the serum from a HC-IgG injected mouse (left panel). Blue = DAPI, green = eGFP, red = anti-human IgG. 63X, scale bar 10 μ m. (C) Continuous spontaneous alternations were reduced in CASPR2-IgG injected mice compared with HC-IgG injected mice ($P = 0.044$) but there was no difference in arm re-entries or in same arm re-entries. (D) In forced alternation, there were no differences in the preference index for number of entries or time spent in the novel arm (NA). (E) Novel object recognition test did not show differences between the two groups in the preference index for the novel object (NO) although there was a trend to reduced preference in CASPR2-IgG injected mice. (F) In the Reciprocal social interaction (RSI) test there was reduced latency to interact ($P = 0.04$; Mann-Whitney test) but no differences in the interaction time, or number of interactions. However, in the non-social aspects of the test, there was increased time spent immobile ($U = 0.008$), reduced rearing ($U = 0.02$) reduced grooming ($U = 0.018$) and longer duration of each grooming bout ($P = 0.002$). (H) The olfaction test showed no differences in the time spent or in the number of visits to the novel odor (NO). Data are expressed as mean \pm SEM with $N = 10$ for CASPR2-IgG injected and $N = 9$ for HC-Injected mice, with the exception of the RSI which was performed on 6 pairs.

Figure 2. Immunoglobulin G in the mouse brains and CASPR2 expression. (A) Representative images of IgG and CASPR2 expression in perfused fixed brains. 40X, scale bar, hippocampus 200 μ m, cerebellum 50 μ m. (B) CASPR2-IgG injected animals had higher levels of IgG in the cortex (Cx) ($P = 0.03$), hippocampus (Hip) ($P = 0.023$) and thalamus (Th) ($P = 0.0004$) compared to HC-IgG injected mice, but not in the cerebellum (Cb) ($N = 4$ /group). No differences were observed in the levels of CASPR2 expression in the same areas (C) ($n = 4$ /group). (D) Moreover, western blots of the whole brains from CASPR2-injected mice showed a trend towards increased CASPR2 expression compared to HC- injected mice (HC) (3 brains/group; means of $N = 4$ replicates for each brain). (E) Representative images of extracellular and intracellular CASPR2-IgG binding on hippocampal neurons dendrites (top), and graph (bottom) showing increase of intracellular puncta

density at 24 h ($P < 0.0001$) in CASPR2-IgG treated neurons without changes in extracellular binding. Scale bar 5 μm .

Figure 3. Effects of IgG on CASPR2-transfected HEK cells. A) Representative images (top) showing IgG in the cytoplasm (green) of HEK cells after 24 h incubation with CASPR2-IgG, without change of the membrane IgG binding (red), confirmed by profile plots (bottom) showing the mean fluorescent intensity for extracellular and intracellular IgG immunostaining across 13 cells. There was some IgG internalisation by 24h. Scale bar 10 μm . B) Representative FACS dot plot of IgG staining on CASPR2-IgG incubated cells (top). Each quadrant represents a cell subpopulation with relative percentages expressed as a number. A trend toward an increase of single stained intracellular (APC positive; top left quadrant) and double positive cells (PE and APC positive; top right) was observed over time along with a reduction of double negative (bottom left) and single stained extracellular cells (bottom right quadrant), particularly at 6 and 16 hours. C) MFI values of extracellular (top) and intracellular (bottom) IgG binding over time in cells incubated in CASPR2-Abs from 3 patients (the transferred and two others with very different CASPR2-Ab titres). No significant differences were detected, but there was a tendency towards an increase of extracellular and intracellular IgG over time. D) Representative FACS dot plot of commercial intracellular (APC) and extracellular (PE) CASPR2 staining on HC-IgG (top) and CASPR2-IgG (bottom) incubated cells. These cells showed no significant differences in the percentage of single intracellular (top left quadrant), double stained (top right quadrant), single extracellular (bottom right quadrant) and double negative (bottom left quadrant) cells. E) MFI values of membrane (top) and intracellular (bottom) CASPR2 staining in HEK cells incubated with HC (N=2) or CASPR2 (N=3) IgG or plasma. No differences were observed in extracellular or intracellular CASPR2 expression over time between the two groups. MFI = mean fluorescence intensity.

Figure 4. Analysis of neurons in mouse brains. (A) Representative pictures of NeuN expression and (B) quantification of NeuN positive cell densities in three brain regions. There were no differences between CASPR2-IgG and HC-IgG injected brains. (C) Calbindin expressing Purkinje cells (PC) were reduced in the cerebellum ($P=0.049$). (D) C-fos expression in the entorhinal-piriform cortex ($P=0.020$), dorsomedial hypothalamus (DMH) ($P=0.037$) and lateral hypothalamus (LH) ($P=0.031$) was higher in the CASPR2-IgG injected compared to the HC-IgG injected mice (Representative images are shown from the entorhinal-piriform cortex). N= 4 brains/group. 40X, 50 μm .

Figure 5. Microglial density and morphological analysis. (A) Representative images of the molecular layer of the cerebellum showing microglia staining. 40X, 20 μm . (B) CASPR2-IgG

injected mice showed higher microglia densities in the somatosensory cortex ($P=0.038$) and in the molecular layer (ML) ($P=0.002$) of the cerebellum but not in the granular layer (GL) or in the hippocampus. $N=4$ animals/group (C) Representative images of the z-stack projected IBA1 staining used for morphological analysis. 40X, 10 μm (D) Quantification of morphological data in the hippocampus and molecular layer of the cerebellum showed that microglia from CASPR2-IgG injected mice had a higher cell soma/cell total body size ratio and shorter ramifications than HC-IgG injected mice, compatible with an activated phenotype in both the hippocampus ($P=0.003$ and $P=0.010$, respectively) and the cerebellum ($P=0.0003$ and $P=0.008$, respectively). 200 cells from 4 animals/groups were analysed from the hippocampus and 100 from the cerebellar molecular layer.

Figure 6. Astrocyte morphology and inflammatory markers. (A) Representative images of GFAP staining in the molecular layer of the cerebellum and quantification of the mean fluorescence intensity in the same area showing higher GFAP expression in the CASPR2-IgG injected mice ($P=0.043$). $N=4$ /group; 40X, 10 μm (B) Representative images of complement C3 expression on GFAP positive cells. Percentage of C3/GFAP area ratio per cell showed that increased C3 expression of astrocytes in the hippocampus ($t(398)=4.87$, $P<0.0001$, 200/cells from 4 animals/group), somatosensory cortex ($t(160)=2.41$, $P=0.01$, 81/cells from 4 animals/group) and cerebellum ($t(204)=7.14$, $P<0.0001$, 103/cells from 4 animals/group) of CASPR2-IgG injected mice. 40X, 10 μm (C) Representative pictures of the z-stack projected GFAP staining used for morphological analysis (40X, 10 μm). The astrocytes from CASPR2-IgG injected mice showed a smaller cell total body size ($U=22052$, $P=0.0051$, 228 cells from 4 animals/group) and shorter ($U=19946$, $P<0.0001$, 228 cells from 4 animals/group) maximal ramification length than HC-IgG injected mice, compatible with an activated phenotype, in the hippocampus. (D) Compared to HC-IgG injected mice, CASPR2-IgG exposed animals showed changes in several cytokines and chemokines, but none reached significance after correcting for multiple comparisons ($N=3$ /group).

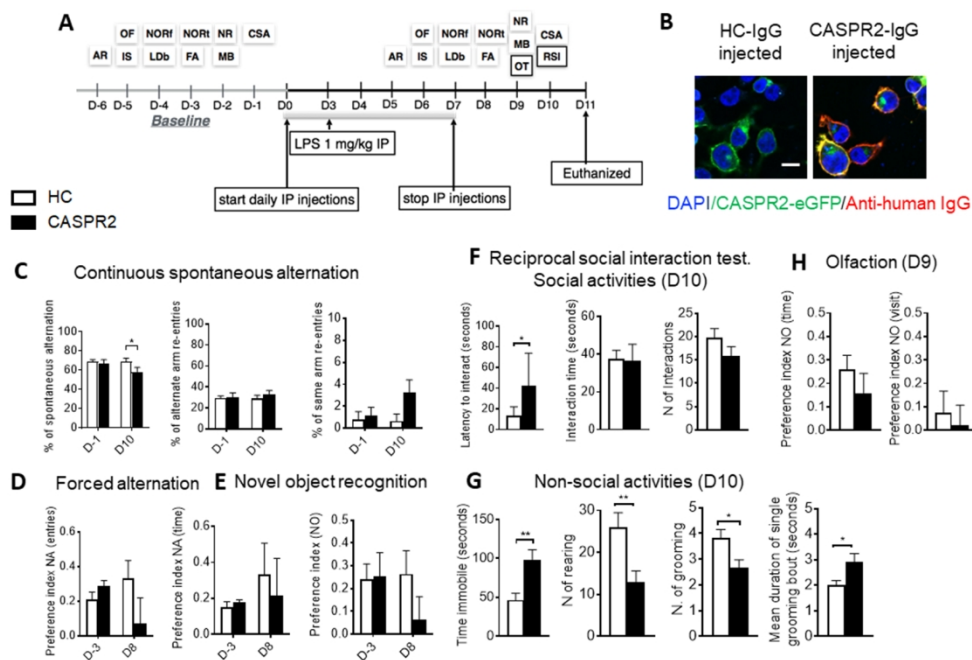


Figure 1. Experimental design and selected behavioural tests. (A) Experimental design. The behavioural tasks assessed locomotion (open field, OF), strength (inverted screen, IS), coordination (accelerating rotarod, AR and narrow beam, NB), working memory (continuous spontaneous alternation, CSA), short-(forced alternation, FA) and long-term memory (novel object recognition, NOR - NORf, familiarization phase, NORr test phase), anxiety (light-dark box, LDb), compulsive-like behaviour (marble burying test, MB), social behavior (reciprocal social interaction tests, RSI) and olfaction (olfaction test, OT). (B) Representative images of cell-based assays showing CASPR2-Ab in the serum from a CASPR2-IgG injected mouse but not in the serum from a HC-IgG injected mouse (left panel). Blue = DAPI, green = eGFP, red = anti-human IgG. 63X, scale bar 10 μ m. (C) Continuous spontaneous alternations were reduced in CASPR2-IgG injected mice compared with HC-IgG injected mice ($P = 0.044$) but there was no difference in arm re-entries or in same arm re-entries. (D) In forced alternation, there were no differences in the preference index for number of entries or time spent in the novel arm (NA). (E) Novel object recognition test did not show differences between the two groups in the preference index for the novel object (NO) although there was a trend to reduced preference in CASPR2-IgG injected mice. (F) In the Reciprocal social interaction (RSI) test there was reduced latency to interact ($P = 0.04$; Mann-Whitney test) but no differences in the interaction time, or number of interactions. However, in the non-social aspects of the test, there was increased time spent immobile ($U = 0.008$), reduced rearing ($U = 0.02$) reduced grooming ($U = 0.018$) and longer duration of each grooming bout ($P = 0.002$). (H) The olfaction test showed no differences in the time spent or in the number of visits to the novel odor (NO). Data are expressed as mean \pm SEM with $N=10$ for CASPR2-IgG injected and $N=9$ for HC-Injected mice, with the exception of the RSI which was performed on 6 pairs.

150x103mm (300 x 300 DPI)

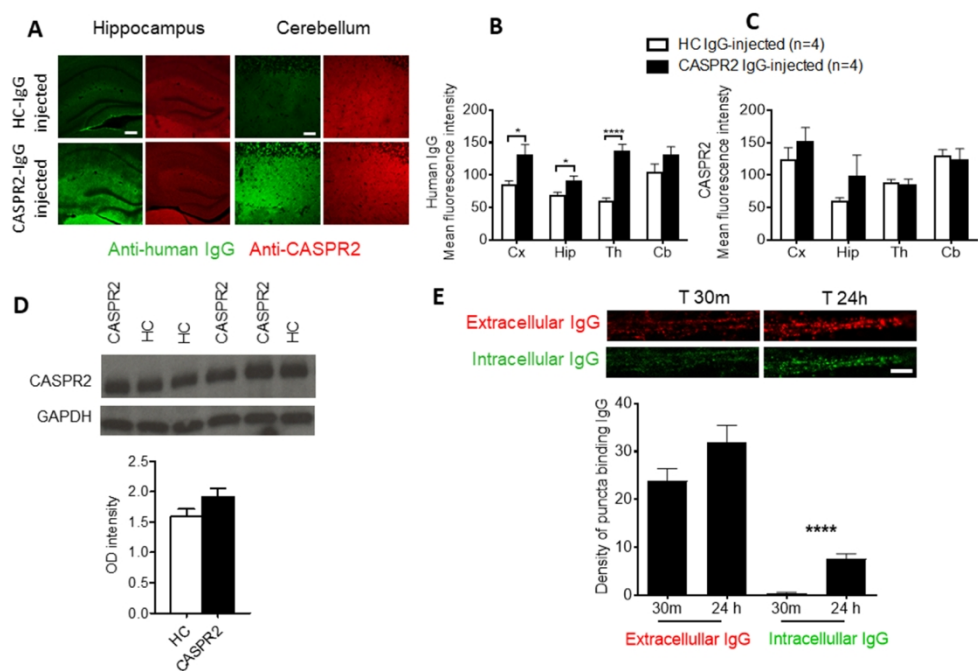
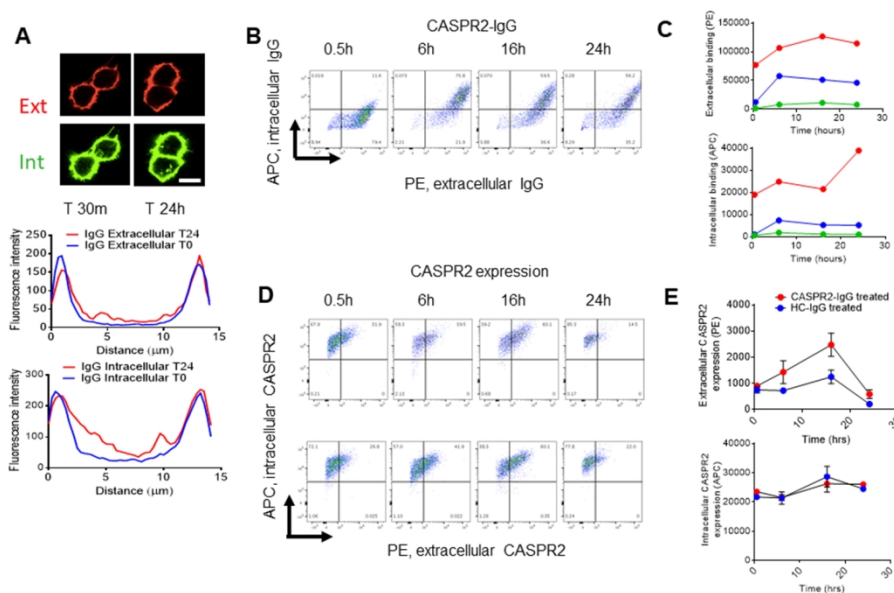


Figure 2. Immunoglobulin G in the mouse brains and CASPR2 expression. (A) Representative images of IgG and CASPR2 expression in perfused fixed brains. 40X, scale bar, hippocampus 200 μ m, cerebellum 50 μ m. (B) CASPR2-IgG injected animals had higher levels of IgG in the cortex (Cx) ($P=0.03$), hippocampus (Hip) ($P=0.023$) and thalamus (Th) ($P=0.0004$) compared to HC-IgG injected mice, but not in the cerebellum (Cb) ($N = 4$ /group). (C) No differences were observed in the levels of CASPR2 expression in the same areas ($N = 4$ /group). (D) Moreover, western blots of the whole brains from CASPR2-injected mice showed a trend towards increased CASPR2 expression compared to HC- injected mice (HC) (3 brains/group; means of $N=4$ replicates for each brain). (E) Representative images of extracellular and intracellular CASPR2-IgG binding on hippocampal neurons dendrites (top), and graph (bottom) showing increase of intracellular puncta density at 24 h ($P < 0.0001$) in CASPR2-IgG treated neurons without changes in extracellular binding. Scale bar 5 μ m.

150x103mm (300 x 300 DPI)



150x103mm (300 x 300 DPI)

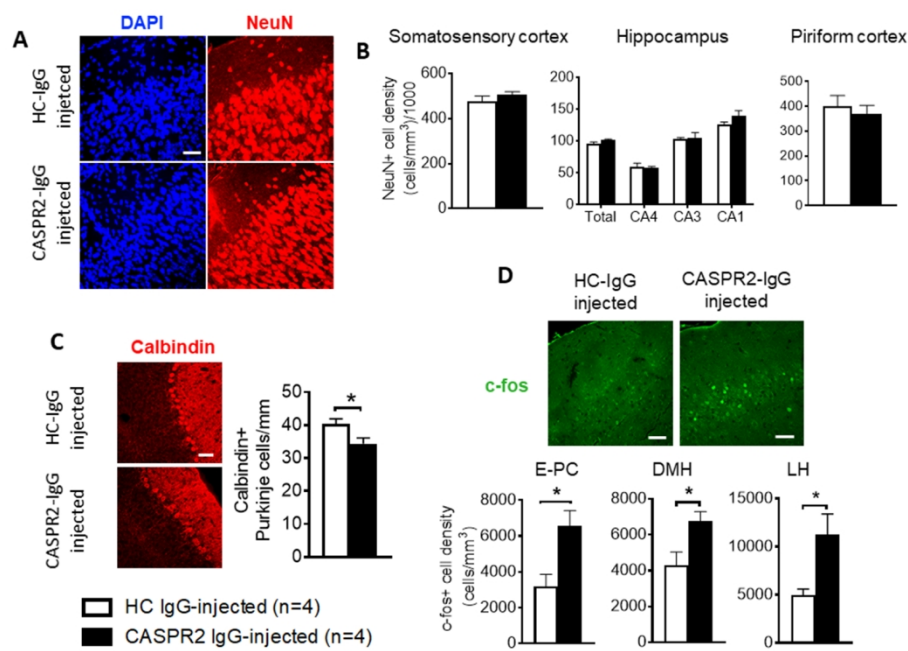


Figure 4. Analysis of neurons in mouse brains. (A) Representative pictures of NeuN expression and (B) quantification of NeuN positive cell densities in three brain regions. There were no differences between CASPR2-IgG and HC-IgG injected brains. (C) Calbindin expressing Purkinje cells (PC) were reduced in the cerebellum ($P=0.049$). (D) C-fos expression in the entorhinal-piriform cortex ($P=0.020$), dorsomedial hypothalamus (DMH) ($P=0.037$) and lateral hypothalamus (LH) ($P=0.031$) was higher in the CASPR2-IgG injected compared to the HC-IgG injected mice (Representative images are shown from the entorhinal-piriform cortex). $N=4$ brains/group. 40X, 50 μm .

150x103mm (300 x 300 DPI)

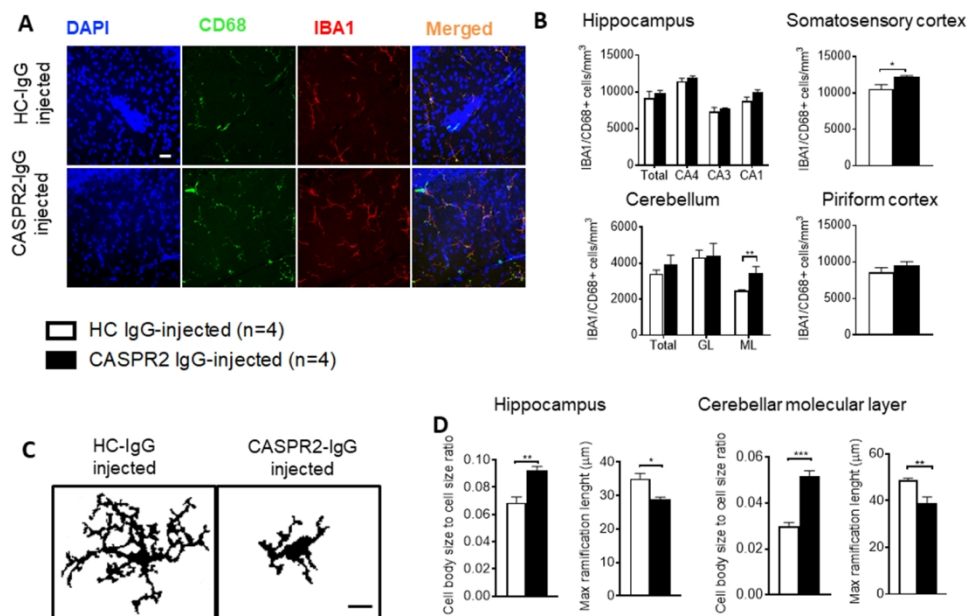


Figure 5. Microglial density and morphological analysis. (A) Representative images of the molecular layer of the cerebellum showing microglia staining. 40X, 20 μm. (B) CASPR2-IgG injected mice showed higher microglia densities in the somatosensory cortex ($P=0.038$) and in the molecular layer (ML) ($P=0.002$) of the cerebellum but not in the granular layer (GL) or in the hippocampus. $N=4$ animals/group (C) Representative images of the z-stack projected IBA1 staining used for morphological analysis. 40X, 10 μm (D) Quantification of morphological data in the hippocampus and molecular layer of the cerebellum showed that microglia from CASPR2-IgG injected mice had a higher cell soma/cell total body size ratio and shorter ramifications than HC-IgG injected mice, compatible with an activated phenotype in both the hippocampus ($P=0.003$ and $P=0.010$, respectively) and the cerebellum ($P=0.0003$ and $P=0.008$, respectively). 200 cells from 4 animals/groups were analysed from the hippocampus and 100 from the cerebellar molecular layer.

150x103mm (300 x 300 DPI)

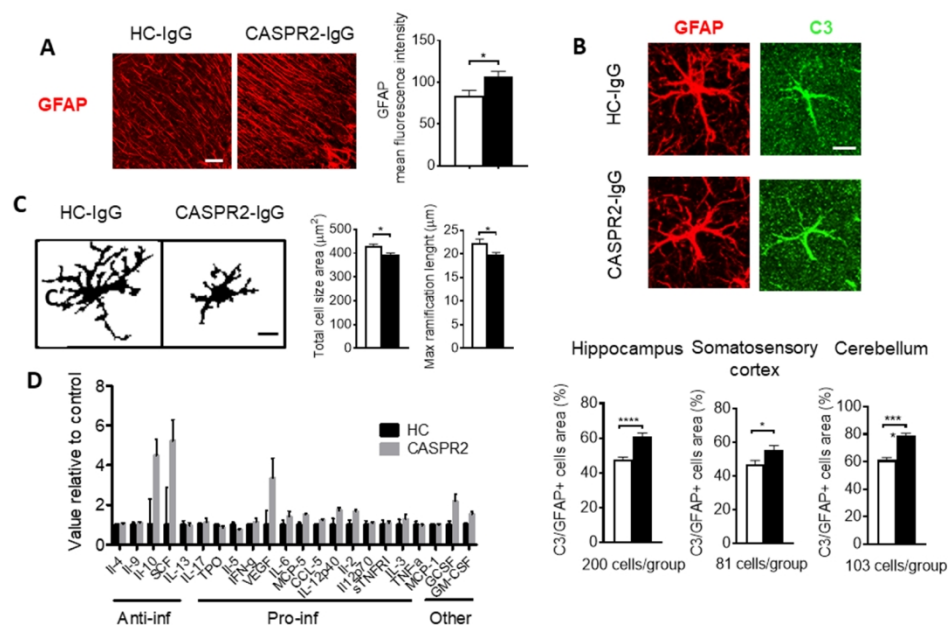


Figure 6. Astrocyte morphology and inflammatory markers. (A) Representative images of GFAP staining in the molecular layer of the cerebellum and quantification of the mean fluorescence intensity in the same area showing higher GFAP expression in the CASPR2-IgG injected mice ($P=0.043$). $N=4/\text{group}$; 40X, 10 μm (B) Representative images of complement C3 expression on GFAP positive cells. Percentage of C3/GFAP area ratio per cell showed that increased C3 expression of astrocytes in the hippocampus ($t(398)=4.87$, $P<0.0001$, 200/cells from 4 animals/group), somatosensory cortex ($t(160)=2.41$, $P=0.01$, 81/cells from 4 animals/group) and cerebellum ($t(204)=7.14$, $P<0.0001$, 103/cells from 4 animals/group) of CASPR2-IgG injected mice. 40X, 10 μm (C) Representative pictures of the z-stack projected GFAP staining used for morphological analysis (40X, 10 μm). The astrocytes from CASPR2-IgG injected mice showed a smaller cell total body size ($U=22052$, $P=0.0051$, 228 cells from 4 animals/group) and shorter ($U=19946$, $P<0.0001$, 228 cells from 4 animals/group) maximal ramification length than HC-IgG injected mice, compatible with an activated phenotype, in the hippocampus. (D) Compared to HC-IgG injected mice, CASPR2-IgG exposed animals showed changes in several cytokines and chemokines, but none reached significance after correcting for multiple comparisons ($N=3/\text{group}$).

Behaviour and neuropathology in mice injected with human contactin- associated protein 2 antibodies

Running title: A passive transfer model of CASPR2 antibodies

Maria Pia Giannoccaro^{1,2}, David A. Menassa^{1,3}, Leslie Jacobson¹, Ester Coutinho¹, Gennaro Prota⁴, Bethan Lang¹, M Isabel Leite¹, Vincenzo Cerundolo⁴, Rocco Liguori^{2,5}, Angela Vincent¹

¹ Nuffield Department of Clinical Neurosciences, University of Oxford, Oxford, UK

² Department of Biomedical and Neuromotor Sciences, University of Bologna, Bologna, Italy

³ Biological Sciences, University of Southampton, Southampton, UK

⁴ MRC Human Immunology Unit, Weatherall Institute of Molecular Medicine, John Radcliffe Hospital, University of Oxford, Oxford, UK.

⁵ IRCSS Istituto delle Scienze Neurologiche di Bologna, Bologna, Italy

Correspondence

Prof Angela Vincent, Nuffield Department of Clinical Neurosciences, University of Oxford, Oxford, UK

Email angela.vincent@ndcn.ox.ac.uk

Tel 07817224849

Supplementary Material 15 pages, 3 figures

Methods

IgG purification and subclass analysis

The plasma from the CASPR2-Ab positive patient and the serum from the healthy donor were centrifuged, diluted 1:1 with Hartmann's solution and incubated with Protein G Sepharose column beads (Sigma-Aldrich, Inc.) overnight at 4 °C on a roller. The Sepharose-IgG mixture was then placed in a glass column before elution of IgG with 0.1M glycine solution (pH 2.3); the eluate was immediately neutralised with 1M Tris pH 8. The protein concentration of the elution was measured using a Coomassie Plus assay kit (Pierce, USA). The eluted fractions were pooled, dialysed against 2 l of Hartmann's physiological solution two times over 24 hours at 4 °C, concentrated by dialysis against polyethylene glycol and filter-sterilized. The concentration was determined using NanoDrop 3300 (ThermoScientific, UK), and IgG was stored at 4 °C.

For CASPR2 antibody subclass analysis, live human embryonic kidney (HEK) cells were incubated with serial dilutions of CASPR2-IgG for 1 hour (h) starting at 1:100 dilution at room temperature (RT) and then fixed with 4% paraformaldehyde (PFA) in phosphate buffered saline (PBS). Binding of antibodies was detected by mouse anti-human IgG1 (Invitrogen, Thermo Fisher Scientific, # MH1013), IgG2 (#05-3500), IgG3 (#05-3600) or IgG4 (MA5-16716) (1:50) antibodies followed by goat anti-mouse IgG-Alexa Fluor® 568 (Thermo Fisher Scientific) conjugated secondary antibody (1:1000). Coverslips were mounted in mounting media (DAKO, Agilent, S3023) containing 4',6-diamidine-2'-phenylindole dihydrochloride (DAPI, Sigma Aldrich) (1:1000). A non-linear visual scoring system was used from 0 to 4. The dilutions of serum at which each subclass crossed the threshold of score 1 was used to calculate the proportion relative to the total.

Behavioural testing

Behavioural testing was done during the light phase. The animals were brought to the experimental room approximately 15 minutes before testing. A rest period of at least 2 hours was allowed between each test. Between mice the walls and the floor of the different apparatus were cleaned with 70% ethanol and dried with a dry tissue.

Accelerating rotarod (AR)

Accelerating rotarod was used to assess motor coordination (Deacon, 2013). The mice were placed on the rotating rod, facing away from the direction of rotation. The rotarod was initially set with a speed of 4 rpm for the initial 10 seconds after which an acceleration of 20 rpm/minute was applied. Time to fall was recorded. If the mouse had fallen off during the initial 10 seconds it would have another try, to a maximum of 3 trials.

Kondziela's inverted screen test (IS) or grip test

This test was used to assess muscle strength. The inverted screen consisted of a 43 caesurae of wire mesh consisting of 12 mm squares of 1 mm diameter wire, surrounded by a 4 cm deep wooden beading to prevent the mice from climbing to the other side. At the beginning of the test the mouse was placed in the centre of the apparatus on the under-side and the screen was quickly inverted while the timer was started. The inverted screen was held 50 cm above a padded surface for a maximum of 5 minutes. The time to fall was recorded. The average of three trials was taken as a final result.

Narrow beams (NB)

Narrow beams or static rods were used as another test of coordination (Deacon, 2013). For this test three wooden rods of varying thickness (35 (rod 1), 22 (rod 2) and 9 (rod 3) mm diameter) each 60 cm long were fixed to a laboratory shelf such that the rods horizontally protrude into space at an height of about 60 cm from a padded floor. The end of the rod near the bench has a mark 10 cm from the end, to denote the finishing line. The mouse was placed at the far end of the widest rod and the timer was started. The orientation time (time taken to orientate 180° from the starting position towards the shelf) and transit time (the time taken to travel to the shelf end) were recorded for a maximum of 5 minutes. If the mouse had not fallen and had arrived at the end of the rod, was transferred on the next smaller rod. If the mouse had not reached the end by this time the test was ended.

Marble burying test (MBT)

This test was used to assess the presence of repetitive, compulsive-like behaviors (Angoa-pérez et al., 2013). Standard polycarbonate mouse cages with fitted filter-top covers were fitted with fresh mouse bedding to a depth of 5 cm and its surface leveled by inserting another cage of the same size onto the surface of the bedding. Ten standard glass toy marbles (assorted styles and colors, 14 mm diameter) were placed on the surface of the bedding in two rows of five marbles. The mouse was placed into a corner of the cage containing the marbles and left undisturbed for 30 min. Food and water access was allowed during the test. At the end of the test the mouse was returned to its home cage and the number of marbles buried counted and expressed as percentage of the total. A marble was scored as buried if two-thirds of its surface area was covered by bedding.

Open field (OF)

The open field was used to assess motricity but also anxiety. The apparatus consisted of a dark closed arena of 50 x 50 cm divided into 10 cm squares illuminated with a 60 W lamp posed 45 cm above the centre of the floor of the box. The mouse was placed in a corner square facing the wall and its movement recorded on camera for 5 minutes. The latency to move, the number of peripheral and central square entered (four paws), the number of rears (both back paws on the ground but not part of grooming), the number of grooming and time spent grooming, the time spent in the peripheral and in the central squares, the time spent moving and the time spent freezing were recorded. The number of faecal boli and the presence/absence of urine were also recorded.

Light-dark box (LDb)

The LD box test was used to assess anxiety. The apparatus consisted of an open white compartment 30 x 20 x 20 cm joined by a 3 x 3 cm opening to a dark box 15 x 20 x 20 cm. The white compartment was illuminated by a 60 W lamp placed 45 cm above the centre of the floor. One side of the white compartment of the box was transparent allowing detection of the mouse movement. The mouse was placed in the middle of the light side facing away from the opening and a count-down timer for 5 min started. The latency to cross with all four paws to the dark side, the latency to cross with all four paws to go back for the first time to the light side, the total time spent on the light side and on the dark side and the number of transitions through the opening were registered for the test. The number of faecal boli and the presence/absence of urine were also recorded.

Forced alternation test (FA) or spatial preference test

This test was used as a measure of short-term memory. The apparatus was a Y-maze constructed from transparent Perspex and mounted on an opaque square Perspex board (64.5 cm x 56.5 cm). The walls of the Y-maze were 20 cm high and 0.5 cm thick. Each arm was 30 cm long and 8 cm wide. The test consisted of 3 periods: a habituation period (5 minutes), a delay period (1 minute) and a test period (2 minutes). During the exposure training trials the entrance to one arm (the Novel arm) was blocked using a rectangular piece of Perspex. The Novel arm was counterbalanced in each group between right and left side. At the start of a trial the mouse was placed at the end of the Start arm (which was always considered as the one closest to the experimenter) and allowed to explore the Start arm and the Other arm. During this period the time spent in each arm and the number of entries to each arm were recorded. An arm entry was defined as when a mouse had placed all four paws into an arm. At the end of the trial the mouse was removed from the maze and returned to its home cage for 1 minute during which the maze was cleaned and the block to the Novel arm removed. At the beginning of the test period the mouse was returned at the end of the Start arm and now allowed to explore the Start, Other, and Novel arms and exploratory behavior assessed for 2 minutes. During the test the time spent in each arm and the number of entries into each arm were recorded. Preference for the Novel arm was calculated as a Preference Index $(\text{entries/time in the new} - \text{entries/time in the old arm}) / (\text{entries/time in the new} + \text{entries/time in the old arm})$ for both the time in arms and number of arm entries (Rubovitch et al., 2010). Scores greater than 0.5 indicate a preference for the Novel arm.

Continuous spontaneous alternation (CSA) test

The continuous spontaneous alternation test was used as a test of working memory. The test was conducted in the same Y-maze as described above and it consisted of a single 5 min trial, in which the mouse was allowed to explore all three arms of the Y-maze. The start arm was varied between animals to avoid placement bias. Spontaneous alternation was assessed by scoring the pattern of entries into each arm during the 5 min of the test. Spontaneous alternation performance (SAP) was defined as successive entries into each of the three arms as on overlapping triplet sets (i.e., ABC, BCA, . . .) and scored as percent of spontaneous alternation (total alternations/total arm entries - 2* 100) (Wietrzych et al., 2005). The percentage of alternate arm re-entries (AARs) (i.e. ABA) and same arm re-entries (SARs) (i.e. AAB) were also scored for each animal in order to assess aspects of attention within spontaneous working memory (Wall and Messier, 2002). Total entries were scored as an index of ambulatory activity in the Y-maze.

Novel object recognition (NOR) test

The novel object recognition test was used to evaluate long term memory (Antunes and Biala, 2012). The open field arena was used in order to benefit from previous habituation. Towers of Lego bricks (X-cm high and X-cm wide) and Falcon tissue culture flasks filled with bedding (9.5 cm high, 2.5 cm deep and 5.5 cm wide, transparent plastic) were used as objects. Animals were randomly assigned one of those pairs of object for the familiarization phase. The test comprised two phases: a familiarization phase (NORf) and a test phase (NORt) performed 24 h later. During the familiarization session two identical objects (either towers of Lego bricks or Falcon tissue culture flasks; the pair was randomized to avoid preference bias) were placed in the open field arena, 5 cm away from the walls. The mouse was placed in the open field, its head positioned opposite the objects, and left free to explore for 5 minutes. The test phase was identical to the familiarization phase but one of the familiar object was replaced in the same position with a new object. The position of the novel object (left or right) was randomized between each mouse. The test was video recorded and subsequently analysed for number of visit and time spent with each object during both the familiarization and the test phase. The object exploration was scored whenever the mouse sniffed the object or touched the object while looking at it (i.e., when the distance between the nose and the object was less than 2 cm). Climbing onto the object (unless the mouse sniffs the object it has climbed on) or chewing the object did not qualify as exploration. If an animal had a total objects exploration time < 5 sec during any phase it was excluded from the analysis. The preference for the new object was expressed as Preference index [PI= (time new object - time familiar object)/(time new object + time familiar object)]. This result can varies from +1 to -1 with a positive score indicating preference for the novel object (Antunes and Biala, 2012).

Reciprocal social interaction test (RSI)

This is a social interaction test where two mice of the same treatment group, unknown to each other, are allowed to interact freely (Barkus et al., 2012). The apparatus was the same used for the open field as the mice were already habituated to it. Two animals from the same treatment group but housed in different cages, tightly matched for weight (within 5% difference) in order to avoid influences on the aggressive behaviour, were exposed to each other for 5 minutes. Six pairs per group were used. To meet the weight criteria one animal for each group was used twice. The test was video recorded and scored offline for the latency to start the interaction and for time spent in social and non-social behaviours and number of social and non-social events. Social behaviours included sniffing, grooming and following closely the other mouse; non-social behaviours included freezing, self-grooming (number of grooming and duration), and rearing.

Olfaction test (OT)

An olfaction test was performed in order to assess olfaction deficits that could interfere with the results from the social interaction test. The open field arena was used in order to benefit from previous habituation. A small plastic container with an odour (1 mL of vanilla or citrus food flavouring) was placed at two corners. The test comprised 3 phases: a sample phase (5 minutes), a delay period (5 minutes) and a test phase (5 minutes). During the first phase, the same odour was placed in both containers (half of the mice for treatment group would smell one odour, while the other half would smell the other). After this, the mice would return to the home cage for 5 minutes. During the test phase, a container with the alternate (new) odour was placed in one of the corners. The location of the new odour was counterbalanced across treatment groups. The test was video recorded and subsequently analysed for number of visit and time spent with each odour.

Ex vivo measurements

CASPR2 cell-based assays

Live cells were incubated with mice' sera for 1 hour (h) starting at 1:100 dilution at room temperature (RT) and then fixed with 4% paraformaldehyde (PFA) in phosphate buffered saline (PBS). Binding of antibodies was detected by goat anti-human IgG-Fc (1:750) (Thermo Fisher Scientific, # 31125) followed by donkey anti-goat IgG-Alexa Fluor® 568 (Thermo Fisher Scientific) conjugated secondary antibody (1:1000). Coverslip were mounted using mounting media (DAKO, Agilent, S3023) containing 4',6-Diamidine-2'-phenylindole dihydrochloride (DAPI, Sigma

Aldrich) (1:1000). A non-linear visual scoring system was used from 0 to 4; samples scoring ≥ 1 were considered positive. The end-point titre of positive samples was calculated by serial dilutions until the reactivity was no longer visible.

Morphological and immunofluorescence analysis of the brain and image processing

Perfused fixed brain sections were cut at 50 μm thickness using a Leica CM1900 cryostat in 10 series. Confocal images were taken of immunofluorescently labeled brain sections using a Zeiss LSM 710 confocal microscope and images were analysed with FiJi software (Open Source HR Software). Brightfield images were taken using the Aperio ScanScope (Leica Biosystem) and analysed in ImageScope (Leica Biosystem) .

Morphological measurements on brain tissue

The presence of gross morphological alterations was evaluated on Nissl-stained sections. Sections were mounted on super frost plus slides (vWR), left to dry at RT, fixed with 4% PFA for 10 minutes, rinsed twice in PBS and once in deionized water for 5 minutes and immersed in cresyl violet solution (Sigma C5042) for 10 minutes. Slides were then dehydrated by immersion in ethanol solutions of increasing concentrations until 100%, cleared with xylene and coverslipped with DPX mounting medium. Slides were scanned with the Aperio AT2 scanner and analysed with the e-pathology Aperio Imagescope image analysis system from Leica Biosystems. The sums of the area of a series of sections (12 sections), from the appearance of the frontal pole cortex to the most posterior part of cerebellum, was multiplied per the number of sections and the thickness of the section (50 μm) to obtain the total brain volume on the coronal plain. The same formula was used to calculate the cerebellum and hippocampus volumes (at least 4 sections). Thickness of the following structures were measured (25-50 measurements per area): anterior cingulate, motor, piriform and somatosensory cortices, neuronal layers of dentate gyrus, CA3 and CA1, CA4, CA3 and CA1 fields, granular and molecular layer of the cerebellum.

Immunostaining of brain tissue

Detection of IgG bound in vivo. To look at the similarity between CAPSR2 staining and IgG staining, two consecutive series were fixed with 4% PFA, washed 3 times in PBS, blocked for 1 h in PBS 10% normal goat serum (NGS) and incubated respectively with anti-human IgG antibodies (Biotium, USA, 20022, 1:500) and with rabbit monoclonal anti-CASPR2 antibodies (Abcam, EPR8738, ab137052, 1:500) in blocking solution overnight at 4°C. Two consecutive sections were

used to avoid any interactions between the secondary anti-human IgG and anti-CASPR2 antibodies. The day after, the sections were washed 3 times in PBS and incubated with goat anti-rabbit Alexa Fluor® 568 secondary (1:500) for 1 h at RT. All sections, including the one incubated with anti-IgG, were washed 3 times in PBS and coverslips were mounted using fluorescent mounting media containing DAPI (1:1000). For quantitative analysis of the mean fluorescent intensity, 32 single plain pictures (4 from the dentate gyrus, 4 from the CA3, 6 from the CA1 areas of the hippocampus, 6 from the somatosensory cortex, 6 from the thalamus, 6 from the cerebellum) were taken from 2 sections per animal. Mean fluorescence intensity was analysed with FiJi software (Open Source HR Software) and results plotted with GraphPad 6 as the mean of the intensity per each area per mouse.

Detection of subpopulations

Neurons and astrocytes were identified by immunofluorescence using a mouse anti-NeuN (Chemicon, MAB377; 1:500) and a polyclonal rabbit anti-glial fibrillary acidic protein (GFAP) antibody (Dako, Z0334; 1:500) respectively. Free-floating sections were fixed with 4% PFA, washed with PBS then blocked with 10% NGS in PBS-Triton-X-100 (0.3%) (PBS-T) for an hour then incubated overnight with primary antibodies at 4°C. The next day the sections were washed in PBS then incubated for two hours at RT with goat anti-mouse (568) and goat anti-rabbit (488) Alexa-fluor secondary antibodies from life technologies at 1:500 dilutions in blocking solution. Sections were subsequently washed in PBS, mounted on slides after a brief wash in TNS (pH = 7.4) and counterstained with DAPI mounting medium, left to dry then sealed and stored protected from the light at 4°C for confocal imaging. Cerebellar sections were stained similarly. In this case, however, primary antibodies included also guinea pig anti-calbindin D28K antibody (Millipore, AB1778; 1:200) for the identification of Purkinje cells. Secondary antibodies included goat anti-mouse (648), goat anti-rabbit (488/568), goat anti guinea pig (555). Neuronal and astrocyte cell densities were determined in the hippocampal fields (CA4, CA3, CA1), the somatosensory cortex and the piriform cortex. Confocal images were taken across the z-plane spanning the entire hippocampus in all cases in both hemispheres. Six images were taken per hemisphere for each cortical region. Eighteen stacks were taken every 2 µm z-plane for the hippocampus. For the neuronal density, cells were counted in every fifth image in the same stack. For astrocyte densities, images were z-projected and cells counted and the density calculated as number of cells per volume of area. In the cerebellum, confocal images were taken across the cerebellar lobules. Fifteen stacks were taken for each case every 3 µm z-plane. To avoid bias related to the different distribution of Purkinje cells across images the Purkinje cell density was calculated as linear density (number of calbindin positive cells per mm). At least 100 cells were counted for each case over 5.3 mm length.

Astrocytes density was assessed in the molecular layer of the cerebellum as mean fluorescence intensity of the GFAP staining. For the neuronal density in the molecular layer, images were z-projected on Fiji and NeuN positive cells counted.

Microglial cells were identified by the combined expression of IBA1 and CD68 markers. Free floating sections were fixed with 4% PFA, washed with PBS then blocked with 10% NGS in PBS-T 0.3% for an hour then incubated overnight with a rat anti-CD68 (BioRad, MCA1957; 1:400) and a rabbit anti-IBA1 (Wako chemicals, 019-19741) primary antibodies in blocking solution at 4°C. The sections were washed the next day with PBS-T 0.3% then incubated for two hours at room temperature with goat anti-rat (488) and goat anti-rabbit (568) Alexa-Fluor® secondary antibodies at 1:500 dilution in blocking solution in the dark. Sections were subsequently washed in PBS, mounted on slides after a brief Tris-NaCl solution (TNS) wash (pH = 7.4) and counterstained with DAPI mounting medium, left to dry then sealed and stored at -20°C for confocal imaging. Quantification of reactive microglia (defined as CD68/IBA-1 positive cells) was performed in the somatosensory and piriform cortex, the CA4, CA3 and CA1 fields of the hippocampus and in the granular and molecular layers of the cerebellum. For each hemisphere, seventeen z-stacks were taken in the hippocampus (3 for the CA4, 4 for the CA3 and 10 for the CA1), nine in the somatosensory area, 4 in the piriform cortex and 5 z-stacks per layer were taken in the cerebellum. The z-step/interval was 2 µm and microglial cells were counted within a 50 µm depth. An average density was obtained (cells/mm³) for each area.

Microglial morphology was assessed in confocal z-stacks detecting fluorescence on IBA-1 expressing cells in the hippocampus and in the molecular layer of the cerebellum as previously described (Coutinho et al., 2017). Soma size (µm²) and total cell body size (µm²) were measured and the soma/total cell body size ratio calculated and used as a marker of microglia activation. The length of the longest ramification (max ramification length) was recorded manually in Fiji.

For C-fos expression, free floating sections were rinsed in TNS, fixed with 4% PFA for 15 minutes then washed 3 times in PBS, blocked for one hour in 10% NGS 0.3% PBS-T and incubated with rabbit anti-cfos (Abcam, ab190289; 1:100) and mouse anti-NeuN (Chemicon, MAB377; 1:500) in blocking solution overnight at 4°C. The day after sections were washed and incubated with goat anti-rabbit (488) and goat anti-mouse (568) Alexa-Fluor® secondary antibodies at 1:500 dilution in blocking solution in the dark at room temperature for two hours. Sections were subsequently washed in PBS, mounted on slides after a brief TNS wash (pH = 7.4) and counterstained with DAPI mounting medium, left to dry then sealed and stored at -20°C for confocal imaging. Quantification

of cfos expressing neurons (defined as cfos/NeunN double-positive cells) was performed in the somatosensory, entorhinal and piriform cortex, the CA4, CA3 and CA1 fields of the hippocampus, the amygdala, the dorso-medial and lateral nuclei of the hypothalamus. For each hemisphere, twelve z-stacks were taken in the hippocampus (3 for the CA4, 4 for the CA3 and 6 for the CA1), four in the somatosensory area, 5 in the entorhinal-piriform cortex, 4 in the amygdala, and 4 z-stacks (2 per subarea) were taken in the hypothalamus. The z-step/interval was 2 μm within a 50 μm depth. An average density was obtained (cells/ mm^3) for each area.

Double staining for complement C3 fraction and GFAP was used to evaluate astrocyte activation. Free floating brain sections were mounted on Superfrost plus slides. When dry, sections were washed with TNS, immersed for 10 minutes in a boiled solution of citrate EDTA buffer and then left in the same solution for 20 minutes on ice. Sections were washed three times in PBS-T 0.3% and incubate with rat anti-C3 (Abcam, EPR19394, ab200999, 1:100) and rabbit anti-GFAP (Dako, 1:500) primary antibodies overnight at 4°C. The day after, sections were washed in PBS-T 0.3% and incubated with goat anti-rat (488) and goat anti-rabbit (568) Alexa-fluor secondary antibodies at 1:500 dilution in 5%NGS PBS-T 0.3% solution in the dark at room temperature for one hour. Slides were then washed in PBS-T 0.3% and TBS, counterstained with DAPI mounting medium, left to dry then sealed and stored at -20°C for confocal imaging. For each hemisphere, three z-stacks were taken in the hippocampus, somatosensory cortex and cerebellum at 40X magnification with a z-step of 2 μm within a 50 μm depth. Images were analyzed using Fiji. After z-projecting and automatic thresholding, the composed images were split in three channels. Images were magnified. Single astrocyte cells were manually selected, and for each cell the area on the GFAP and on the C3 channels measured. For each cells the C3 expression was calculated as C3/GFAP stained cell areas ratio. 200 cells/group were analyzed in the hippocampus, 81 cells/group in the somatosensory cortex and 100 cells/group in the cerebellum, and the results plotted as cells average/group average. Astrocytes morphology was assessed on the same z-stacks detecting fluorescence in GFAP expressing cells using the same script as for assessing microglia morphology (Countinho E et al 2017). The total cell body size (μm^2) was measured and the number of ramifications and the length of the longest ramification (max ramification length) were recorded manually in Fiji.

Cellular infiltration of B and T lymphocytes was assessed using rat anti-CD19 (Abcam, 1:100, ab25232) and rabbit anti-CD3 (Abcam, 1:100, ab16669) antibodies, respectively. Free floating brain sections were rinsed in TNS, fixed with 4% PFA for 10 minutes than washed 3 times in PBS, blocked for one hour in 10% NGS 0.3% PBS-T and incubated with primary antibodies in blocking solution overnight at 4°C. The day after sections were washed and incubated with goat anti-rat

(488) or goat anti-rabbit (568) Alexa-Fluor® secondary antibodies at 1:500 dilution in blocking solution in the dark at room temperature for one hour. Sections were subsequently washed in PBS, mounted on slides after a brief TNS wash (pH = 7.4) and counterstained with DAPI mounting medium, left to dry then sealed and stored at -20°C for confocal imaging.

Immunoblot and cytokine analyses

For total brain protein extraction, frozen brain tissue (3 brain and cerebellar hemispheres per mice/group) was homogenate in lysis buffer (50 mM TRIS-HCL, 150 mM NaCl, 0.1% SDS, 1% triton-X 100, pH 7.4) supplemented with protease inhibitors (1:100) with a mechanical homogenizer. The homogenate was then spun at 17000 rpm for 20 minutes at 4°C. Supernatant was collected and protein concentration measured by a Pierce™ BCA protein assay kit (23225).

For western blot (WB) analysis, NuPAGE sample reducing agent (10x; Invitrogen, NP0009) and LDS sample buffer (4x; Invitrogen,) were added to 10 to 30 µg of an appropriate amount of solubilized tissue, boiled for 10 minutes and the proteins separated into 3-8%Tris acetate SDS polyacrylamine gels (Invitrogen, NP0322) and transferred with dry blotting on nitrocellulose membranes. Membranes were blocked in 5% non-fat skimmed milk in PBS 0.1% Tween 20 solution and incubated overnight at 4°C with rabbit anti CASPR2 (Abcam, EPR8738, ab137052, 1:1000) and anti-GAPDH antibodies (Abcam, [EPR16891] ab181602 1:2000). Membranes were washed in PBS-Tween 0.1% and incubated with secondary antibodies in blocking solution for 1 h at room temperature (anti-rabbit IgG HRP 1:1000). Signals were detected by enhanced chemiluminescence (Amersham GE Healthcare) and captured on autoradiography film (GE Healthcare). All studies were done in duplicate or triplicate. Films were digitally scanned and signals quantified using Fiji ImageJ software. The signal intensity of each antigen was normalized to that of GAPDH in the same lane.

Brain cytokine expression was analyzed using a Mouse Cytokine Antibody Array (22 Targets) (Abcam, ab133993) as per manufacturer instructions. Briefly, membranes were blocked in blocking buffer for 30 minutes at room temperature then incubated with 250 of proteins from the brain lysate in blocking buffer overnight at 4°C. The day after, membranes were thoroughly washed and incubated with biotin-conjugated anti-cytokines antibodies overnight at 4°C. Following washing, streptavidin-HRP was applied for 2 hours at room temperature. Immunoreactivity was then visualized using enhanced chemiluminescence reagent. X-ray film was then scanned and densitometric analysis performed using Fiji. Positive controls were included on each membrane and

used for results normalization. The mean intensity of the normalized signal in HC-IgG injected mice was defined as 1 and the other intensities expressed relatively to this value.

In vitro studies on CASPR2 expression and internalisation in neurons and HEK cells

To evaluate the effects of CASPR2 antibodies in vitro, we initially assessed the presence of internalisation by evaluating surface and intracellular human CASPR2-IgG binding at time 0 and after 24 h rat hippocampal neurons and on transfected HEK cells by immunofluorescence analysis. Subsequently, transfected HEK cells were used to evaluate changes in CASPR2-IgG binding and CASPR2 expression over time using flow cytometry (FACS).

Hippocampal primary rat neurons (Kaech S and Banker G 2006) (DIV12) were incubated for 30 minutes or 24 h with either HC- or CASPR2-IgG (1:200) at 37°C, followed by washing and incubation with goat anti-human IgG 568 (1:1000) in blocking solution (1% BSA) for 30 minutes at RT. Coverslips were washed and fixed with 4% PFA and, after further washing, incubated with goat anti-human IgG 488 (1:1000) for further 30 min in PBS-0.3% triton, before mounting with DAPI. Confocal images were thresholded and analysed with SynPAnal software. For each image, 50 µm axonal segments were manually traced, and the puncta density automatically quantified for each segment.

HEK cells were transfected with CASPR2 cDNA. Sixteen hours after transfection, the media was replaced with media supplemented with either HC- or CASPR2-IgG (1:200). Cells were washed either 30 min (T0) or 24 h (T24) after exposure to the IgG and live cells immediately incubated with goat anti-human IgG 568 (1:1000) in blocking solution (1% BSA) for 30 minutes. Coverslips were washed and fixed with 4% PFA and, after further washing, incubated with goat anti-human IgG 488 (1:1000) for further 30 min in PBS-0.3% triton, before mounting with DAPI. Confocal photographs were taken at 63x magnification (10 fields/coverslip). Using ImageJ software, profile plots of each cell were made spanning the cell diameter for both the intracellular and the extracellular IgG immunoreactivity and the signal intensity was then averaged for the portion of the plot relating the membrane and for the one relating the cytoplasm.

For FACS, HEK cells were transfected with CASPR2-EGFP cDNA. Sixteen hours after transfection the media was replaced with media supplemented with either HC- (1 subject) or CASPR2- IgG (1 case) or plasma (2 patients with CASPR2 antibodies and 1 HC). Cells were washed either 30 min (T0), 6 (T6), 16 (T16) or 24 h (T24) after exposure to the IgG, detached and

seeded in V-bottom 96 well plates. Live cells were immediately incubated with goat anti-human IgG 568 (1:1000) in blocking solution (1% BSA) for 30 minutes or with mouse anti-CASPR2 (abcam, 1:200, 105581) followed by Alexa-Fluor goat anti mouse 568 for 30 minutes. Cells were washed, incubated 10 min with live/dead near infrared antibodies (Invitrogen), fixed with 4% PFA and, after further washing, incubated with either goat anti-human IgG 633 (1:1000) or with rabbit anti-CASPR2 (abcam, 1:200, ab33994) followed by goat anti-rabbit 647 for further 30 min in PBS-0.3% triton. After further washing cells were resuspended in PBS for flow cytometry cell acquisition. Compensation controls, i.e. unstained transfected HEK293 cells, were included in the analysis. Samples were acquired with a Fortessa X50 flow cytometer (BD biosciences), and analysed with FlowJo (Tree Star) gating on live cells. The percentage of cells stained only for APC (intracellular IgG) or PE (extracellular IgG) or for both (double positive) and the unstained (double negative) and the mean fluorescence intensity (MFI) for each time-point were analysed.

References

Angoa-pérez, M. et al. (2013) 'Marble Burying and Nestlet Shredding as Tests of Repetitive, Compulsive-like Behaviors in Mice', (December), pp. 1–7. doi: 10.3791/50978.

Antunes, M. and Biala, G. (2012) 'The novel object recognition memory: Neurobiology, test procedure, and its modifications', *Cognitive Processing*, 13(2), pp. 93–110. doi: 10.1007/s10339-011-0430-z.

Barkus, C. et al. (2012) 'GluN1 hypomorph mice exhibit wide-ranging behavioral alterations', *Genes, Brain and Behavior*, 11(3), pp. 342–351. doi: 10.1111/j.1601-183X.2012.00767.x.

Coutinho, E. et al. (2017) 'Persistent microglial activation and synaptic loss with behavioral abnormalities in mouse offspring exposed to CASPR2-antibodies in utero', *Acta Neuropathologica*. Springer Berlin Heidelberg, 134(4), pp. 567–583. doi: 10.1007/s00401-017-1751-5.

Deacon, R. M. J. (2013) 'Measuring Motor Coordination in Mice', *Journal of Visualized Experiments*, (75), pp. 1–8. doi: 10.3791/2609.

Kaech S, Banker G (2006). 'Culturing hippocampal neurons', *Nat Protoc*, 1(5), pp. 2406-15.

Rubovitch, V. et al. (2010) 'The intricate involvement of the Insulin-like growth factor receptor signaling in mild traumatic brain injury in mice', *Neurobiology of Disease*. Elsevier Inc., 38(2), pp. 299–303. doi: 10.1016/j.nbd.2010.01.021.

Wall, P. M. and Messier, C. (2002) 'Infralimbic kappa opioid and muscarinic M1 receptor interactions in the concurrent modulation of anxiety and memory', *Psychopharmacology*, 160(3), pp. 233–244. doi: 10.1007/s00213-001-0979-9.

Wietrzyk, M. et al. (2005) 'Working memory deficits in retinoid X receptor γ -deficient mice', *Learning & Memory*, 12(3), pp. 318–326. doi: 10.1101/lm.89805.et.

Figure legends

Supplementary figure legends

Supp. Fig 1: Behavioral testing in mice exposed to HC- or CASPR2-IgG. All data are represented as CASPR2-IgG vs HC-IgG mean \pm SDs in the text but shown as mean \pm SEM in the Figures. A) Weights over time: no differences between HC and CASPR2-IgG injected animals (group $P = 0.83$, time \times status $P = 0.35$, repeated measure ANOVA). B) Accelerating rotarod (AR): no differences in the time to fall between groups ($t(17)=0.93$, $P=0.36$, unpaired t-test; 307.8 ± 150.3 vs 260.1 ± 27.9). C) Inverted screen (IS): no differences in time to fall between groups ($F(1,16) = 3.8$, $P = 0.06$, one-way ANCOVA; 227.3 ± 42.2 vs 269.6 ± 48.8). D) Narrow beam test, on the smallest beam: no differences between groups in orientation time ($F(1,17) = 0.03$, $P = 0.95$, two-way mixed ANOVA; 9.6 ± 7.9 vs 6.2 ± 3) or in transit time ($F(1,17) < 0.001$, $P = 0.98$, two-way mixed ANOVA; 63.9 ± 95 vs 49.7 ± 94.5). E) Marbles burying test (MB) no differences between groups in percentage of marbles buried ($F(1,16) = 0.52$, $P = 0.47$, one-way ANCOVA; 36 ± 24.1 vs 37.7 ± 21). F) Open field: no differences in number of central entries ($F(1,16) = 0.11$, $P = 0.73$, one-way ANCOVA; 4 ± 4 vs 5.1 ± 3.4), number of rearing ($F(1,16) = 2.53$, $P = 0.13$, one-way ANCOVA; 14.7 ± 15 vs 11.3 ± 6.4), number of grooming ($F(1,16) = 0.39$, $P = 0.54$, one-way ANCOVA; 2.9 ± 2.1 vs 2.4 ± 0.8) or time spent immobile ($F(1,16) = 1.1$, $P = 0.31$, one-way ANCOVA; 135.8 ± 48 vs 156 ± 51.4) between the two groups. G) Light-dark box: no differences between groups in latency to move to the dark side of the box ($F(1,16) = 1.05$, $P = 0.32$, one-way ANCOVA; 5.2 ± 2.4 vs 6.7 ± 3.4), time spent in the dark ($F(1,16) = 0.13$, $P = 0.71$, one-way ANCOVA; 268.3 ± 20.6 vs 267.4 ± 22) and number of crossings between the two chambers ($F(1,16) = 0.14$, $P = 0.71$, one-way ANCOVA; 7.6 ± 5 vs 7 ± 3.7).

Supplementary figure 2. Nissl staining. A) Photograph showing the cresyl violet staining of a brain serie (left panel) and volumetric measurements. No differences were observed in brain volume ($P=0.20$, unpaired t-test; 307.4 ± 34.7 vs 276.2 ± 7.7), cerebellar ($P=0.29$, unpaired t-test; 30.6 ± 3.9 vs 27.1 ± 3.1) and hippocampal volumes ($P=0.63$, unpaired t-test; 8.8 ± 0.99 vs 9.2 ± 1.2) between HC-IgG and CASPR2-IgG injected mice. B) Cortical thickness measurements. No differences were observed in the thickness of the anterior cingulate cortex ($P=0.80$, unpaired t-test; 751.6 ± 32.5 vs 758.9 ± 47.2), primary motor cortex ($P=0.91$; 1044 ± 115.7 vs 1036 ± 87.5), although a tendency towards a reduced thickness was noted in the piriform cortex of CASPR2-IgG injected animals compared to controls ($P=0.073$; 441.7 ± 20.8 vs 484 ± 33). C) Photograph showing an example of cortical layers measurement in the somatosensory cortex and quantification of the layers thickness. No differences were observed in the thickness of layer 1 ($P=0.46$; 87.2 ± 15 vs 76.3 ± 23.6), layers 2-4 ($P=0.83$; 406.6 ± 70.3 vs 415.2 ± 39.9) and layers 5-6 ($P=0.84$; 588.6 ± 78.4 vs 577.6 ± 77.5) between animals. D) Photograph showing an example of hippocampal cell body layers and fields measurements and their quantification. No differences were observed in the thickness of dentate gyrus (DG) ($P=0.96$; 63.5 ± 5.7 vs 63.4 ± 4.6), CA3 ($P=0.84$; 58.9 ± 3.4 vs 59.7 ± 5.4) and CA1 ($P=0.35$; 57.9 ± 5.7 vs 54.1 ± 8) nor in the thickness of CA4 ($P=0.56$; 192.7 ± 8.1 vs 183.3 ± 13.3), CA3 ($P=0.65$; 121.2 ± 16.3 vs 128.4 ± 34.7) and CA1 ($P=0.04$, not significant after Holm-Sidak correction for multiple comparison; 384.3 ± 32.7 vs 348.9 ± 17.4). E) Quantification of the thickness of cerebellar layers. No differences were observed between groups in the thickness of the granular ($P=0.70$; 145.9 ± 11.5 vs 150.4 ± 2.3) and molecular ($P=0.32$; 158.7 ± 8.6 vs 170.9 ± 12.9) layers of the cerebellum. Data are expressed as mean \pm SEM; N= 4 brains/group.

Supplementary figure 3. Representative microphotographs of CD19 (top, green) and CD3 (bottom, red) staining in the parenchyma of CASPR2-IgG injected mice. Scale bar 20 μ m.

Behaviour and neuropathology in mice injected with human contactin- associated protein 2 antibodies

Running title: A passive transfer model of CASPR2 antibodies

Maria Pia Giannoccaro^{1,2}, David A. Menassa^{1,3}, Leslie Jacobson¹, Ester Coutinho¹, Gennaro Prota⁴, Bethan Lang¹, M Isabel Leite¹, Vincenzo Cerundolo⁴, Rocco Liguori^{2,5}, Angela Vincent¹

¹ Nuffield Department of Clinical Neurosciences, University of Oxford, Oxford, UK

² Department of Biomedical and Neuromotor Sciences, University of Bologna, Bologna, Italy

³ Biological Sciences, University of Southampton, Southampton, UK

⁴ MRC Human Immunology Unit, Weatherall Institute of Molecular Medicine, John Radcliffe Hospital, University of Oxford, Oxford, UK.

⁵ IRCSS Istituto delle Scienze Neurologiche di Bologna, Bologna, Italy

Correspondence

Prof Angela Vincent, Nuffield Department of Clinical Neurosciences, University of Oxford, Oxford, UK

Email angela.vincent@ndcn.ox.ac.uk

Tel 07817224849

No. Words 5089

No. Pages 22

No. Figures 6

No. Tables 0

Supplementary Material 15 pages, 3 figures

Abstract

Serum antibodies (Abs) that bind to the surface of neurons or glia are associated with a wide range of rare but treatable CNS diseases. In many, if not most instances, the serum levels are higher than CSF levels yet **most of** the reported attempts to reproduce the human disease in mice have used infusion of Abs into the mouse cerebral ventricle(s) or intrathecal space. We used the intraperitoneal (ip) route and injected purified plasma IgG from either a CASPR2-Ab positive patient (n = ten mice) or healthy individual (n = nine mice) daily for 8 days. Lipopolysaccharide was injected ip on day 3 to cause a temporary breach in the blood brain barrier. A wide range of baseline behaviours, including tests of locomotion, coordination, memory, anxiety and social interactions, were established before the injections and tested from day 5 until day 11. At termination, brain tissue was analysed for human IgG, CASPR2 and c-fos expression, **lymphocyte infiltration**, and neuronal, astrocytic and microglial markers. Mice exposed to CASPR2-IgG, compared with control-IgG injected mice, displayed reduced working memory during the continuous spontaneous alternation test with trends towards reduced short-term and long-term memories. In the open field tests, activities were not different from controls, but in the reciprocal social interaction test, CASPR2-IgG injected mice showed longer latency to start interacting, associated with more freezing behaviour and reduced non-social activities of rearing and grooming. At termination, neuropathology showed more IgG deposited in the brains of CASPR2-IgG injected mice, but a trend towards increased CASPR2 expression; **these results were mirrored in short-term in vitro experiments where CASPR2-IgG binding to hippocampal neurons and to CASPR2-transfected HEK cells led to some internalisation of the IgG, but with a trend towards higher surface expression. Despite these limited results, in the mouse brains** there was increased c-fos expression in the piriform-entorhinal cortex and hypothalamus, and a modest loss of Purkinje cells. In the CASPR2-IgG injected mice, there was also increased microglia density, morphological changes in both microglia and astrocytes and raised complement C3 expression on astrocytes, all consistent with glial activation. Patients with CASPR2- Abs can present with a range of clinical features reflecting central, autonomic and peripheral dysfunction. Although the behavioural changes in mice were limited to social interactions and mild working-memory defects, the neuropathological features indicate potentially widespread effects of the antibodies on different brain regions.

Keywords (5): CASPR2 antibodies, animal model, passive transfer, microglia activation, astrocytes

Abbreviations: Ab, antibodies; AR, accelerating rotarod; BBB, blood-brain barrier; CASPR2, Contactin-associated protein 2; CCL5, Chemokine (C-C motif) ligand 5; CD68, cluster of differentiation 68; CSA, continuous spontaneous alternation; DAPI, 4',6-diamidin-2-fenilindolo; DRG, dorsal root ganglia; ECL, enhanced chemiluminescence; eGFP, enhanced green fluorescent protein; FA, forced alternation; GCSF, granulocyte-colony stimulating factor; GFAP, glial fibrillary acidic protein; GM-CSF, granulocyte-macrophage colony-stimulating factor; HC, healthy control; HRP, horseradish peroxidase; IBA1, ionized calcium-binding adapter molecule 1; ICV, intracerebroventricular; IFN- γ , interferon gamma; IgG, immunoglobulin G; IL, interleukin; Ip, intraperitoneally; IS, inverted screen; LDb, light-dark box; LPS, lipopolysaccharide; MB, marble burying test; MCP-1, monocyte chemoattractant protein-1; MCP-5, monocyte chemoattractant protein-5; NA, novel arm; NB, narrow beam; NeuN, neuronal nuclei; NO, novel object/odor; NOR, novel object recognition test; NORf, novel object recognition familiarization phase; NORt, novel object recognition test phase; OF, open field; OT, olfaction test; PBS, perfused with phosphate-buffered saline; PC, Purkinje cells; PFA, paraformaldehyde; RSI, reciprocal social interaction tests; SDS, sodium dodecyl sulphate; SCF, stem cell factor; sTNFRI, Soluble tumor necrosis factor receptor I; TNF α , tumor necrosis factor alpha; TPO, thrombopoietin; TRIS- HCL, tris(hydroxymethyl)aminomethane hydrochloride; VEGF, vascular endothelial growth factor.

Introduction

Antibodies directed against contactin-2 associated protein 2 (CASPR2-Abs) have been associated with a wide range of peripheral (neuromyotonia, pain and autonomic dysfunction) and central nervous system (CNS, cognitive impairment, memory loss, insomnia, hallucinations, delusions, ataxia and epilepsy) symptoms (Irani et al., 2010). In addition, CASPR2-Abs were found in archived gestational sera from mothers whose offspring had neurodevelopmental disorders (Coutinho et al., 2017a); this situation was modelled in a maternal to-fetal transfer study that showed autistic-like behaviour and neuropathological alterations in the offspring of dams injected with CASPR2-Abs (Coutinho et al., 2017b). The effects of several antibodies, most notably those against the NMDA receptor, have been modelled by intraventricular injection (eg. Planagumà et al., 2015; Wright et al., 2015) but there have been no reports of the pathogenicity of CASPR2-Abs in the CNS of adult mice.

CASPR2-Abs are typically at higher titres in serum than in CSF (Sonderen et al., 2016; Bien et al., 2017). Intraperitoneal (ip) injection of purified immunoglobulin G (IgG) from two CASPR2-Abs positive patients to mice over 18 days reduced the thresholds for mechanical stimuli and enhanced the excitability of dorsal root ganglia (DRG) neurons through reductions in Kv1 potassium channel expression but, in that study, brain pathology was not investigated in detail (Fig S3 in Dawes et al., 2018). To explore the effects of CASPR2-Abs in the CNS, we used a similar protocol with 8 daily injections of IgG purified from one patient with autoimmune encephalitis and from one healthy control. We added a single dose of lipopolysaccharide (LPS) at day 3 to disrupt the blood-brain barrier (BBB). We evaluated the effects of the antibodies on mouse behaviours from day 5 of the injections and for 3 days following the last one, and subsequently examined brain pathology.

Although previous studies have used a peripheral approach to study antibodies to synaptic vesicle proteins (eg. Amphiphysin, Sommer C et al., 2005; GAD, Chang et al., 2013) this is the first transfer of antibodies to a cell-surface neuronal antigen.

Material and methods

Purification of human IgG

Immunoglobulin G were purified using Protein G Sepharose beads (Sigma, P3296) from a plasma exchange sample of a 71-year old male patient with CASPR2-related encephalitis (CASPR2-IgG) and from sera of one healthy age- and sex-matched individual (HC-IgG) as previously described

(Dawes et al., 2018). The subclasses of the CASPR2-IgG antibodies were determined on the purified IgG (see Supplementary material).

Experimental design and behavioural testing

Animals

The nineteen C57Bl6 male mice aged 6 weeks (18-22 g) were from a licensed breeding establishment (Charles River). The animals were housed in groups of four or five under standard laboratory conditions (ad libitum access to food and water; 12:12 light:dark cycle, with lights on at 7:00) and monitored daily during the experimental period. Mice were tagged and randomly assigned to each experimental group. All in vivo experiments were performed in the Biomedical Services Unit at the John Radcliffe Hospital in accordance with the United Kingdom Home Office Animals in Scientific Procedures Act (1986) and with institutional guidelines. All in vivo and in vitro experiments were performed with animals or tissue coded.

The experimental design is summarised in Fig. 1A. Mice were injected intraperitoneally (ip) daily with either CASPR2-IgG (ten mice, 20 mg/ml Day 0 (D0) and 12 mg until D8) or HC-IgG (nine mice, 20 mg/ml D0, 12 mg D1-2 and 6 mg/ml until D8). At day 3 all animals were injected ip with LPS (1 mg/Kg from E. Coli O111.B4, L3012, Sigma Aldrich, UK). At day 11 animals were sacrificed.

Behavioural tasks were performed according to standardized tests (eg. Coutinho et al., 2017b) blind to the animal status and following the schedule summarized in Fig. 1A. All tests, with the exception of the reciprocal social interaction and the olfactory tests, were performed for up to 5 days before D0 and from D5 till D11 during and after the IgG injections. A description of each task is provided in the Supplementary Material.

Blood and brain tissue processing

At day 11, eleven animals (6 CASPR2-IgG and 5 HC-IgG injected) were randomly selected and sacrificed by CO₂. Blood samples were collected by cardiac puncture, centrifuged and the sera were stored at -20°C before testing by cell-based assay for CASPR2-IgG (see Supplementary Material). Brains were harvested and snap-frozen for protein extraction. The remaining eight animals (4/group) were perfused with phosphate-buffered saline (PBS) followed by ice-cold 4% paraformaldehyde (PFA). Brains were removed, post-fixed, cryoprotected with 30% sucrose in PBS and snap-frozen. All brains were stored at -80 °C.

Morphological and immunofluorescence analysis of the brain

Neuropathological studies were performed as previously described (Coutinho et al., 2017b) and are detailed in Supplementary Material. PFA-perfused fixed brain sections were cut at 50 μm thickness using a Leica CM1900 cryostat. Confocal images were taken of immunofluorescently labeled brain sections using a Zeiss LSM 710 confocal microscope and images were analysed with FiJi software (Open Source HR Software). Brightfield images were taken using the Aperio ScanScope (Leica Biosystem) and analysed in ImageScope (Leica Biosystem). To evaluate gross morphology, sections were Nissl-stained with Cresyl Violet (C5042, Sigma Aldrich, UK).

To look at the similarity between CASPR2 and IgG staining, two consecutive series were incubated with anti-human IgG antibodies (Biotium, 20022, 1:500) and with rabbit monoclonal anti-CASPR2 antibodies (Abcam, UK, Ab137052, 1:500) respectively.

Neurons and astrocytes were identified by immunofluorescence using anti-NeuN (Merck, MAB377, 1:500) and anti-glial fibrillary acidic protein (GFAP) (Dako, 203334, 1:500) respectively. For neuronal c-fos, sections were co-stained with anti-c-fos (Abcam, ab190289, 1:100) and anti-NeuN antibodies. In the cerebellum, anti-calbindin D28K antibody (Millipore, AB1778; 1:200) was used for the identification of Purkinje cells (PC). Astrocyte morphology was assessed in GFAP expressing cells and also by co-staining for complement C3 (Abcam, Ab200999, 1:100).

Microglial density was measured with anti-IBA1 (Wako chemicals, 019-19741, 1:500) and anti-CD68 (BioRad, MCA1957; 1:400) markers. Soma size (μm^2), total cell body size (μm^2) and the soma/total cell body size ratio was used to assess microglial activation, as previously described (Coutinho et al., 2017). Cellular infiltration of B and T lymphocytes was assessed using the CD19 (Abcam, 1:100, ab25232) and the CD3 (Abcam, 1:100, ab16669) antibody markers, respectively.

Immunoblot analysis

Whole brains (3 per group) were homogenised in lysis buffer (50 mM TRIS-HCL, 150 mM NaCl, 0.1% SDS, 1% triton-X 100, pH 7.4) supplemented with protease inhibitors (1:100) and applied to SDS-polyacrylamide gels, transferred to nitrocellulose membranes and probed with rabbit anti-CASPR2 (Abcam, ab137052, 1:1000) and anti-GAPDH antibodies (Abcam, ab181602, 1:2000) followed by HRP-coupled secondary antibody. Antibody binding was detected by enhanced chemiluminescence (ECL) (Amersham GE Healthcare) and captured on autoradiography film (GE Healthcare). Films were scanned and signals quantified using Fiji ImageJ software. Each brain

extract was tested four times and the mean intensities of signal for CASPR2-IgG mice was compared with the mean intensities of HC-IgG mice.

Brain cytokine expression was analyzed using a Mouse Cytokine Antibody Array (22 Targets) (Abcam, 133993) as per the manufacturer's instructions. Immunoreactivity was then visualized using ECL and analysed using Fiji as above. Positive controls were included on each membrane and used for normalisation. Because of the range of different values for each test substance, the CASPR2-IgG intensities were expressed relative to the signal for the HC-IgG intensities (as in Dawes et al., 2018).

In vitro experiments

To look in more detail at the effects of CASPR2-Abs, hippocampal neurons and CASPR2-transfected HEK cells were exposed to CASPR2-IgG and HC-IgG for between 30 mins to 24 hours at 37 C. The binding of IgG to the surface of unpermeabilised cells, and presence of IgG intracellularly in fixed permeabilised cells, was measured by confocal microscopy and flow cytometry (FACS). FACS was used to measure CASPR2 expression using an extracellular (Abcam, UK, 105581) and an intracellular (Abcam, UK, ab33994) anti-CASPR2 commercial antibody (both 1:200). Details of the methods are given in Supplementary material.

Statistics

A student's t-test or a Mann-Whitney were used for comparison between groups as appropriate. Holm-Sidak was applied to correct for multiple comparisons. Behavioural data were analysed by one-way ANCOVA, using the baseline as a covariate, or with two-way mixed ANOVA. Transformations were applied if necessary to meet normality or to adjust for inequality of variances. Repeated measure ANOVA or two-way mixed ANOVA was performed on flow cytometry data. Significance was placed at $P < 0.05$. Statistical tests were carried with IBM SPSS statistics version 20.0 (SPSS Inc., Chicago, USA). Data in the text are presented as mean \pm SDs, CASPR2-IgG vs HC-IgG mice. Graphs are plotted as mean \pm SEMs (Graph Pad prism version 6, GraphPad software, San Diego, California, USA).

Results

CASPR2-IgG injected mice have mild cognitive and behavioural impairments

Exposure to most of the behavioural tests was performed during the 5 days preceding the start of the injections; testing was then conducted during the injections (D5-7) and for the 3 days following the final injection (D8-10) (see Fig 1A). A cell-based assay for CASPR2-Abs confirmed high levels in the CASPR2-IgG injected mice even on Day 11, 4 days after the last IgG injection (Fig 1B). Body weights over the period of the experiment, motor tests (accelerating rotor-rod, inverted screen, multiple narrow beams) and tests of anxiety (open field, light-dark box test) at D5-9 showed no differences between the two groups (Supplementary Material Fig. 1). These observations suggested no effect of the CASPR2-Abs on general health or well-being.

There were differences, however, between CASPR2-IgG and HC-IgG injected mice with respect to cognitive and social activities. The following results are given as mean \pm SD, CASPR2-IgG vs HC-IgG unless otherwise stated. The CASPR2-IgG injected mice showed reduced numbers of spontaneous alternations at D10 ($F(1,16) = 4.75$, $P = 0.04$, partial $\eta^2 = 0.22$, two-way mixed ANOVA; 55 ± 10.9 vs 68.8 ± 10.3 (with one outlier removed); Fig. 1C) suggestive of a working memory impairment. This finding was supported by the 50% of CASPR2-IgG injected mice that showed same arm re-entries compared with 11% of HC-IgG injected. CASPR2-IgG injected mice also showed trends towards a reduced preference index for entries in the new arm in the forced alternation task at Day 8 ($F(1,16) = 3.36$, $P = 0.085$; 0.07 ± 0.46 vs 0.33 ± 0.3 ; Fig. 1D), and reduced preference index ($F(1,16) = 2.45$, $P = 0.14$; 0.06 ± 0.32 vs 0.26 ± 0.25 ; Fig. 1E) in the novel object recognition test on D10.

Social and non-social behaviours were tested by the reciprocal social interaction test on D10. CASPR2-IgG injected mice showed longer latency to start interacting compared to HC-IgG injected mice ($U = 5.5$, $P = 0.04$; Mann-Whitney test U, Fig. 1F; 41.9 ± 78 vs 13.4 ± 21.2) but similar interaction time and number of interactions. In non-social activities (Fig. 1G), including grooming and locomotor activity, CASPR2-IgG injected animals showed less exploratory behaviour with longer time spent immobile ($t(22) = 3.42$, $P = 0.002$; t-test; 98.6 ± 43.2 vs 46.6 ± 30.1) and reduced rearing ($t(22) = 3.01$, $P = 0.006$; t-test; 13 ± 8.8 vs 26 ± 12) compared to HC-IgG injected animals. In addition, the CASPR2-IgG injected group had reduced grooming events ($t(22) = 2.61$, $P = 0.015$; t-test; 2.6 ± 1 vs 3.8 ± 1.1), but a longer duration of each self-grooming bout ($t(22) = 2.48$, $P = 0.002$; t-test; 2.9 ± 1.1 vs 2 ± 0.6). Equivalent non-social behaviors had been assessed during the open field and no differences were observed between groups (Supplementary Material Fig. 1), suggesting that the changes shown in Figure 1G reflected an influence of the social context. Importantly, olfactory function, which can influence social activities, was similar in the two groups on D9 (Fig. 1H).

CASPR2-IgG accesses the brain but does not alter CASPR2 expression

The distribution of human IgG was investigated in different brain regions by immunofluorescence (Fig. 2A). The level of deposited IgG was higher in the cortex ($t(6)=2.71$, $P=0.03$, t-test; mean fluorescence intensity (MIF): 130.9 ± 31.6 vs 85.3 ± 11.1), hippocampus ($t(6)=3.03$, $P=0.023$, t-test; 92.2 ± 12.4 vs 68.8 ± 9.1), and thalamus ($t(6)=7.14$, $P=0.0004$, t-test; 137.3 ± 20 vs 61 ± 7.3) of CASPR2- IgG injected mice compared to controls (Fig. 2A,B). Nevertheless, there were no apparent differences in CASPR2 expression, measured by a commercial anti-CASPR2 antibody, between the two groups in these areas (Fig. 2A and 2C), or when total CASPR2 protein was quantified by western blot (WB) in whole brain lysates, where there was a trend towards increased CASPR2 expression ($t(6)=1.7$, $P=0.13$; optical density (OD): 1.9 ± 0.2 vs 1.5 ± 0.2 ; Fig. 2D).

Effects of CASPR2-IgG antibodies in vitro

Although the absence of CASPR2 loss mirrored previous in vitro findings (Patterson et al., 2018), the effects of CASPR2-IgG were further explored in vitro. First, we measured the subclasses of the CASPR2 antibodies as these are relevant to the potential mechanisms. Although mostly IgG4 (72%), there was also IgG1 (22%) and a little IgG2 (6%); IgG3 was <1% of the total. We then looked at the effects on rat hippocampal cultured neurons. After 24 h incubation with CASPR2-IgG, an increase in intracellular IgG ($t(28)=7.02$, $P < 0.0001$, unpaired t test with Welch's correction; puncta density T 30 min vs T 24h: 0.46 ± 0.17 vs 7.66 ± 1 total 71 segments examined from 2 experiments) was observed without a reduction of the density of extracellular puncta (Fig 2E), suggesting some internalisation of the IgG. To pursue further we studied CASPR2 IgG or HC IgG binding to CASPR2-transfected HEK cells and IgG internalisation by confocal imaging. After 24 h incubation, live cells were stained with anti-human IgG 568 (red) secondary antibodies, then fixed, permeabilised and stained again with anti-human IgG 488 (green) secondary antibodies. There was no apparent loss of surface IgG binding but evidence of cytoplasmic IgG aggregates; this was demonstrated graphically by profile plots of mean fluorescence intensity across the cells that showed the presence of cytoplasmic IgG after 24 h incubation with CASPR2-IgG without, however, significant changes in the membrane IgG binding (Fig 3A). These results were confirmed by analysis of the fluorescence intensity of the IgG on the membrane and in the cytoplasm: membrane IgG was unchanged over time whereas intracellular IgG was increased at 24 h compared to 30 min ($t(55)=3.10$, $P=0.003$, unpaired t test with Welch's correction; MFI at 30m vs 24h: 35.08 ± 2.3 vs 54.95 ± 5.9 , $N=102$ cells from 2 experiments).

To confirm these findings, we repeated the experiment using flow cytometry (FACS). In this case we also used two additional CASPR2-Abs patients and one more control. Examples are shown in Figure 3B and results summarised in Fig 3C. Although not significant, there was an increase in extracellular IgG binding as shown by an increase in the percentage of double-stained cells (Fig 3B upper right quadrant) and MFI values ($F(1.6, 3.3)=5.4$, $P=0.09$, repeated measure ANOVA with Greenhouse-Geisser correction; Fig. 3C, top) over the first few hours, that plateaued by 6-16 hours. Intracellular IgG was found in a variable proportion of the CASPR2-IgG bound cells between the three patients ($F(1.09, 2.31)=1.4$, $P=0.35$, repeated measure ANOVA with Greenhouse-Geisser correction), roughly correlating with IgG bound extracellularly (Fig 3C, bottom). We also looked in parallel at CASPR2 expression using an extracellular CASPR2 antibody and an intracellular CASPR2 antibody (Fig 3D). The extracellular antibody showed a trend towards increased levels over the first 16 hours in CASPR2-IgG compared with HC-IgG treated cells ($F(1,4)=3.1$, $P=0.14$, two-way mixed ANOVA) (Fig 3E, top); thereafter, extracellular CASPR2 expression declined in both CASPR2 and HC-IgG treated cells. By contrast, there was no difference between CASPR2 expression using the intracellular CASPR2 antibody between HC-IgG and CASPR2-IgG patients at any time point ($F(1,4)=0.16$, $P=0.7$, two-way mixed ANOVA) (Fig 3E bottom).

CASPR2-IgG exposure does not cause generalised neuronal loss

No gross morphological changes were observed on Nissl-stained sections between the two groups for hippocampal, cerebellar and total brain volume. The thickness of the cortical (anterior cingulate, primary motor, somatosensory, piriform cortices), hippocampal and cerebellar layers was also not different (Supplementary Material Fig 2).

Densities of NeuN-positive neurons were measured in the somatosensory, piriform cortex, hippocampus and cerebellum. No evidence of neuronal loss was found in the CASPR2-IgG compared to the HC-IgG injected mice in the cortical areas or in the hippocampus (Fig. 4A, B). In the cerebellum, however, despite no difference in the count of NeuN positive cells in the molecular layer, there was a 14.6% reduction in the number of calbindin-positive Purkinje cells ($t(6)=2.45$, $P=0.049$, t-test; 34.3 ± 3.4 vs 40.2 ± 3.3) (Fig. 4C).

C-fos expression is a marker of neuronal activity and was measured on NeuN stained neurons. Compared to the HC-injected mice, mice injected with CASPR2-IgG showed a higher density of c-fos expressing neurons in the entorhinal-piriform cortex ($t(6)=3.11$, $P=0.020$, t-test; 6574 ± 1694 vs 3167 ± 1389), dorsomedial ($t(6)=2.67$, $P=0.036$; t test; 6743 ± 1090 vs 4304 ± 1462) and lateral

($t(6)=2.79$, $P=0.031$, t test; 11238 ± 4313 vs 4955 ± 1277) hypothalamus (Fig. 4D). No differences between groups in the density of c-fos expressing neurons were detected in the hippocampus, somatosensory cortex and amygdala.

CASPR2-IgG injected mice display microglial activation and increased microglia density

Activated microglial cells, as identified by expression of IBA1 and CD68 (Fig. 5A), were measured in the somatosensory and piriform cortices, the hippocampus and the cerebellum. Microglial density was increased in the somatosensory cortex of CASPR2-IgG injected mice ($t(6)=2.63$, $P=0.038$, t test; 12169 ± 355 vs 10550 ± 1177) and molecular layer of the cerebellum ($t(6)=4.99$, $P=0.002$, t test; 3432 ± 378.5 vs 2481 ± 35.2) but not in the piriform cortex, the hippocampus or the granular layer of the cerebellum (Fig. 5B).

Analysis of microglial morphology was performed on IBA1 positive cells (Fig. 5C) in the hippocampus and in the molecular layers of the cerebellum. When activated, microglia assume an ameboid morphology characterized by a larger soma body and shorter processes. In the hippocampus, microglia from CASPR2-IgG injected mice showed a higher cell soma/cell total body size ratio ($t(6)=4.74$, $P=0.0032$, t -test; 0.092 ± 0.005 vs 0.068 ± 0.008), less ($t(6)=3.27$, $P=0.017$, t -test; 4 ± 0.1 vs 4.28 ± 0.1) and shorter ($t(6)=3.68$, $P=0.010$, t -test; 29.04 ± 0.9 vs 35.07 ± 3.1) ramifications than HC-IgG injected mice, compatible with an activated phenotype. Similar results were found in the molecular layer of the cerebellum, with a higher soma/total body area size ratio ($t(6)=7.35$, $P=0.0003$, t -test; 0.051 ± 0.004 vs 0.029 ± 0.003) and shorter ramification maximal length ($t(6)=3.68$, $P=0.008$, t -test; 39.08 ± 4.8 vs 48.87 ± 1.4) than HC-IgG exposed mice (Fig. 5D); no significant difference was seen in the number of ramifications.

CASPR2-IgG injected mice display astrocytic activation without overt astrocytosis

There were no differences in the density of GFAP-positive cells in the somatosensory and piriform cortices, or in the hippocampus (data not shown) but increased GFAP expression in the molecular layer of the cerebellum ($t(6)=2.55$, $P=0.043$, t -test; MFI 106.7 ± 12.5 vs 83.97 ± 12.7) (Fig. 6A). Nevertheless, there was evidence of reactive astrocytosis as indicated by complement C3 and GFAP co-expression. The C3/GFAP co-stained area was raised in CASPR2-IgG injected mice in the hippocampus ($t(398)=4.87$, $P<0.0001$, 200/cells per group, t -test; 60.69 ± 32.6 vs 47.88 ± 17.8), somatosensory cortex ($t(160)=2.41$, $P=0.01$, 81/cells per group, t -test; 55.53 ± 24.2 vs $47.07 \pm$

20.09) and cerebellum ($t(204)=7.14$, $P < 0.0001$, 103/cells per group, t-test; 78.99 ± 16.8 vs 61.19 ± 18.8) (Fig. 6B). The astrocytes from CASPR2-IgG injected mice also showed a smaller cell total body size ($U=22052$, $P=0.0051$, 228/cells per group Mann Whitney test U; median CASPR2- vs HC-IgG: 366.9 vs 397.8) and shorter ($U=19946$, $P < 0.0001$, Mann Whitney test U; median CASPR2- vs HC-IgG: 18.67 vs 21.06) maximal ramification length than HC- IgG injected mice, compatible with an activated phenotype, in the hippocampus (Fig. 6C).

As these microglial and astrocyte changes suggested a state of mild neuroinflammation in the CASPR2-IgG injected mice, we assessed the presence of B and T cells infiltrates. CD19- and CD3- positive cells were sparse and observed mainly in the meninges and choroid plexus, and only very rarely in the parenchyma (Supplementary Figure 3). Additionally, a commercial cytokine/chemokine array was performed on three whole brain lysates from each group to look for changed neuroinflammatory markers. A trend towards increased levels was noted for several cytokines and chemokines, and particularly for interleukin (IL)-10, stem cell factor (SCF), and vascular endothelial growth factor (VEGF), but none reached significance after correction for multiple comparisons (Fig. 6D).

Discussion

Many of the recently-described antibody-mediated CNS diseases have higher serum antibodies than CSF antibody levels, emphasizing that in many or most cases they are likely to be initiated by a peripheral immune response. It was timely, therefore, to see whether peripheral injection of antibodies could, under conditions where the blood brain barrier is briefly compromised, lead to evidence of CNS dysfunction. CASPR2-Ab at very high serum titers have been identified in patients with both peripheral and central neurological disorders. Here we showed that, after intraperitoneal (ip) injection of CASPR2-IgG with one dose of lipopolysaccharide, the antibodies reached the mouse brain parenchyma, and were associated with mild changes in cognitive and in socially-dependent non-social behaviours; the mouse brains showed increased activated microglia and astrocytes and increased c-fos expression, but no evidence of neuronal loss or reduction in CASPR2 expression.

Previous studies showed that LPS is able to breach the BBB (Kowal et al., 2004; Banks et al., 2015) and allow peripherally administered antibodies to penetrate the brain parenchyma without causing, *per se*, sustained neurotoxicity or neuroinflammation (Kowal et al., 2004). We used a single injection of LPS during a peripheral passive transfer of IgG into adult mice, similar to that used in many previous studies on peripheral disorders (Fukunaga et al., 1983; Piddlesden et al., 1996;

Viegas et al., 2012), and recently sensory hypersensitivity (Dawes et al., 2018). Human IgG was present in the brain of both control and CASPR2-IgG injected mice, as would be expected after LPS but, in all areas except the cerebellum, the intensity was higher in the CASPR2-IgG injected mice.

Most antibody-mediated diseases act, at least partially, by antigenic modulation by which the antibodies cross-link and internalise their target, but we found no reduction of CASPR2 expression on immunohistology. A recent study in vitro found that CASPR2-Abs did not reduce CASPR2 expression on the surface of cultured hippocampal neurons, but that they inhibited the interaction of CASPR2 with its extracellular binding partner, contactin2 (Patterson et al., 2018). In vivo, CASPR2-Abs reduced the surface expression of Kv1 on DRG neurons (Dawes et al., 2018) but specific mechanism was not studied. In the current model, we cannot exclude that by the time the neuropathology was performed, on day 11, compensatory mechanisms may have occurred to restore CASPR2 expression. Indeed, a trend towards higher levels of CASPR2 levels was seen in the brain extracts of CASPR2-IgG injected mice, and our in vitro neuronal and HEK experiments, also showed a trend towards higher levels of CASPR2 surface expression after 6-16 hours exposure to CASPR2 antibodies, as well as some IgG internalisation, which was not investigated in the previous study (Patterson et al., 2018). Thus it appears that some CASPR2-IgG is internalised, which would be expected because of the presence of IgG1 divalent antibodies in the CASPR2-IgG preparation; but apparently this was not sufficient to cause loss of CASPR2 from the cell surface and the trend towards higher CASPR2 expression, both in vivo and in vitro, suggests that there might be some compensatory changes.

Behaviourally, during the social interaction test CASPR2-IgG injected mice showed longer latency to interact but otherwise normal sociability. However, they showed increased immobility and anxiety-like behaviour and, since the same non-social activities were normal during other tests (i.e. open field), these behaviours are likely to be related to the social novelty context (Meeker et al., 2013). This interpretation is also supported by the longer grooming bout during the same test (Kaluff and Tuohimaa, 2004). These observations need to be explored in more detail in the future.

CASPR2-IgG injected mice showed less alternation in the continuous spontaneous alternation tests, with similar trends in the forced alternation and novel object recognition tests. These findings might seem inconsistent with the lack of histological changes in the hippocampus. However, although working memory is related to hippocampal integrity, other brain areas play a role in these tasks (Lalonde, 2002). Among those, the entorhinal cortex, where CASPR2 is highly expressed (Gordon et al., 2016), is the main source of hippocampal afferents from the neocortex and is involved in

different forms of memory (van Groen et al., 2003). Indeed, in mouse models of Alzheimer's disease, memory impairment was associated with an early hyper-excitability of the entorhinal cortex (Xu et al., 2015) which would be consistent with increased neuronal excitability following reduction in Kv1 expression which was seen in the dorsal root ganglia in the peripheral CASPR2-Ab model (Dawes et al., 2018).

These changes may also have been responsible for the higher levels of c-fos expression in the entorhinal-piriform cortex, rather than in the hippocampus. Interestingly, increased c-fos expression was also observed in the dorsomedial and lateral hypothalamus. The lateral hypothalamus is related to the sleep-wake cycle, with increased levels of c-fos expression during the dark period, when the mice are active (Basheer et al., 1997). Thus, an increase of c-fos expression during the light period in our animals might suggest an increased wakefulness, consistent with the insomnia typically observed in patients with Morvan's Syndrome (Liguori et al., 2001). Clearly, further experimental studies on the effects of CASPR2-Ab on sleep are also needed.

Consistently with previous findings (Dawes et al., 2018), CASPR2-Ab did not cause evident neuronal loss, except in the cerebellum, where there was a mild loss of Purkinje cells. CASPR2-Abs bind to the axons of granule cerebellar neurons in the molecular layer and have been associated with cerebellar ataxia in some patients (Becker et al., 2012), as well as with morphological changes of Purkinje cells in a neuropathological case (Sundal et al., 2017). The only 14.6% loss of these cells might explain why we did not observe coordination difficulties in the mice in the accelerating rotarod or narrow beam.

One striking finding was the activation of microglia and astrocytes. Microglia and astrocytes are responsible for the innate immunity in the brain and their functions are strictly interconnected. Previous studies showed that in pathological conditions (Lian et al., 2016; Liddelow et al., 2017), activated microglia were able to induce reactive astrocytes, which up-regulate C3 expression and become responsible for neurotoxicity and loss of synapses. Accordingly, alongside microglia activation and increased density, we found increased C3 expression on the surface of astrocytes and higher numbers of activated astrocytes in CASPR2-IgG injected mice. The microglial and astrocytic activation was particularly evident in the cerebellum where reactive microglia have been associated with PC loss in a mouse model of cerebellar degeneration (Zhao et al., 2011). Finally, although there were no significant changes in cytokine or chemokine expression when examined at termination, even after correction for multiple comparisons there were trends towards increased levels of those relevant to glial activity. **The lack of an overt inflammatory response was further**

supported by the absence of B and T cells infiltrates in the brain parenchyma, in accordance with previous findings in the spinal cord (Dawes et al., 2018).

Microglial activation has been reported in neuropathological cases of patients with CASPR2-Ab encephalitis (Körtvelyessy et al., 2015; Sundal et al., 2017). Moreover, microglial activation and increased density was noted in cortex of animals exposed to CASPR2-Abs in utero and this activation persisted into adulthood (Coutinho et al., 2017b). By contrast, the peripheral administration of CASPR2-IgG, without LPS, induced only a mild increase of microglia in the spinal cord but not in the somatosensory cortex of exposed animals (Dawes et al., 2018), suggesting that the microglial activation in this model is dependent on the effects of CASPR2-IgG in the brain.

Our study has several limitations. First, we used whole IgG rather than cloned CASPR2-IgG antibodies. The purified IgG did not bind to CASPR2-null mouse brain tissue (Coutinho et al., 2017b) and the results of transfer from mother to offspring of the IgG were similar to those obtained with a monoclonal CASPR2 antibody (Brimberg et al., 2017). It was concluded that the effects seen were largely or only due to the CASPR2 specific antibodies. Second, only one case and one control were studied and unfortunately the yield of control serum IgG was limited and not sufficient to match the CASPR2-IgG over the full course of the injections, although the amounts were matched until the LPS injection. Third, the experimental timing we chose could mean that we missed the acute effects of the antibodies while some behavioural and histological effects might have required more time to become fully established. Fourth, the use of LPS, could have induced additional inflammation and contributed to determining the site of BBB disruption, leading to, or changing, some of the antibody effects we observed. However, previous studies in our laboratory and elsewhere have shown that IgG penetration into the brain in the absence of LPS is low (Braniste et al., 2014) and that LPS is necessary to produce an effective transfer to the brain parenchyma (Kowal et al., 2004). Moreover, in a similar transfer experiment with glutamic-acid decarboxylase antibodies and two doses of LPS (Chang et al 2012), any human IgG bound was restricted to hippocampus and brain stem areas, compared to the wider distribution seen here for CASPR2-IgG antibodies. The alternative approach of intracerebroventricular (ICV) injection of the antibodies would have overcome the need to use LPS to open the BBB, but there is no evidence yet that the ICV approach provides a more complete model of autoimmune disorders such as NMDAR-Ab encephalitis (Planagumà et al., 2015; Wright et al., 2015), since in neither case were there movement disorders or spontaneous seizures seen in the NMDAR-Ab infused mice. Nevertheless, as there is little understanding about the relative roles of CSF and serum antibodies in some of these conditions, a direct comparison between the peripheral and intraventricular approaches could be

very interesting. Finally, many questions remain unanswered such as the full mechanisms by which CASPR2-Abs affect brain, whether the glial changes are relevant to the human disease, and if they are dependent on the specificity of the antibody or common to all forms of autoimmune encephalitis.

Despite the limitations, our findings demonstrate that peripherally administered CASPR2-Abs, in the presence of a temporary breach in the BBB, are able to access the brain and produce histological and behavioural changes. These data support a pathogenic role of CASPR2-IgG in mediating the CNS symptoms observed in patients with encephalitis and lead the way for more detailed studies on how and where the antibodies act to cause the full range of clinical features.

Acknowledgements

We are very grateful to Prof D Bannerman for his advice regarding behavioural testing, and to Prof David Bennett, Drs Steven West and John Dawes for advice regarding the confocal measurements.

Funding

There was no specific funding for this study. MPG was supported by the Department of Biomedical and Neuromotor Sciences, University of Bologna. EC was funded by the Programme for Advanced Medical Education, Fundação Calouste Gulbenkian. We are very grateful to the Nuffield Department of Clinical Neurosciences for their contributions to the further support of the project (MPG, LJ, DM, BL).

Conflict of interest

The University of Oxford holds patents for LGI1, CASPR2 and Contactin2 antibodies, licensed to Euroimmun AG for antibody assays. AV and BL receive a proportion of royalties.

References

Banks WA, Gray AM, Erickson MA, Salameh TS, Damodarasamy M, Sheibani N, et al. Lipopolysaccharide-induced blood-brain barrier disruption: Roles of cyclooxygenase, oxidative stress, neuroinflammation, and elements of the neurovascular unit. *J. Neuroinflammation* 2015; 12: 1–15.

Basheer R, Sherin JE, Saper CB, Morgan JI, McCarley RW, Shiromani PJ. Effects of sleep on wake- induced c-fos expression. *J. Neurosci.* 1997; 17: 9746–9750.

Becker EBE, Zuliani L, Pettingill R, Lang B, Waters P, Dulneva A, et al. Contactin-associated protein-2 antibodies in non-paraneoplastic cerebellar ataxia. *J. Neurol. Neurosurg. Psychiatry* 2012; 83: 437–440.

Bien CG, Mirzadjanova Z, Baumgartner C, Onugoren MD, Grunwald T, Holtkamp M, et al. Anti-contactin-associated protein-2 encephalitis: relevance of antibody titres, presentation and outcome. *Eur. J. Neurol.* 2017; 24: 175–186.

Braniste V, Al-Asmakh M, Kowal C, Anuar F, Abbaspour A, Tóth M, et al. The gut microbiota influences blood-brain barrier permeability in mice. *Sci Transl Med.* 2014; 6:263ra158.

Brimberg L, Mader S, Jeganathan V, Berlin R, Coleman TR, Gregersen PK, et al. Caspr2-reactive antibody cloned from a mother of an ASD child mediates an ASD-like phenotype in mice. *Mol Psychiatry.* 2016; 21: 1663-1671.

Chang T, Alexopoulos H, McMenamin M, Carvajal-González A, Alexander SK, Deacon R, et al. Neuronal surface and glutamic acid decarboxylase autoantibodies in Nonparaneoplastic stiff person syndrome. *JAMA Neurol.* 2013; 70: 1140-9.

Coutinho E, Jacobson L, Pedersen MG, Benros ME, Nørgaard-Pedersen B, Mortensen PB, et al. CASPR2 autoantibodies are raised during pregnancy in mothers of children with mental retardation and disorders of psychological development but not autism. *J Neurol Neurosurg Psychiatry.* 2017a; 88: 718-721.

Coutinho E, Menassa DA, Jacobson L, West SJ, Domingos J, Moloney TC, et al. Persistent microglial activation and synaptic loss with behavioral abnormalities in mouse offspring exposed to CASPR2-antibodies in utero. *Acta Neuropathol.* 2017b; 134: 567–583.

Dawes JM, Weir GA, Middleton SJ, Patel R, Chisholm KI, Pettingill P, et al. Immune or Genetic-Mediated Disruption of CASPR2 Causes Pain Hypersensitivity Due to Enhanced Primary Afferent Excitability. *Neuron* 2018; 97: 806–822.e10.

Fukunaga H, Engel AG, Lang, B, Newsom Davis J, Vincent A. Passive transfer of Lambert-Eaton myasthenic syndrome with IgG from man to mouse depletes the presynaptic membrane active zones. 1983; 80: 7636–7640.

Gordon A, Salomon D, Barak N, Pen Y, Tsoory M, Kimchi T, et al. Expression of Cntnap2 (Caspr2) in multiple levels of sensory systems. *Mol. Cell. Neurosci.* 2016; 70: 42–53.

van Groen T, Miettinen P, Kadish I. The entorhinal cortex of the mouse: Organization of the projection to the hippocampal formation. *Hippocampus* 2003; 13: 133–149.

Irani SR, Alexander S, Waters P, Kleopa KA, Pettingill P, Zuliani L, et al. Antibodies to Kv1 potassium channel-complex proteins leucine-rich, glioma inactivated 1 protein and contactin-associated protein-2 in limbic encephalitis, Morvan's syndrome and acquired neuromyotonia. *Brain* 2010; 133: 2734–2748.

Kalueff A V., Tuohimaa P. Grooming analysis algorithm for neurobehavioural stress research. *Brain Res. Protoc.* 2004; 13: 151–158.

Körtvelyessy P, Bauer J, Stoppel CM, Brück W, Gerth I, Vielhaber S, et al. Complement-associated neuronal loss in a patient with CASPR2 antibody-associated encephalitis. *Neurol. Neuroimmunol. NeuroInflammation* 2015; 2: e75.

Kowal C, DeGiorgio L a., Nakaoka T, Hetherington H, Huerta PT, Diamond B, et al. Cognition and Immunity. *Immunity* 2004; 21: 179–188.

Lalonde R. The neurobiological basis of spontaneous alternation. *Neurosci. Biobehav. Rev.* 2002; 26: 91–104.

Lian H, Litvinchuk XA, Chiang AC, Aithmitti N, Jankowsky JL. Astrocyte-Microglia Cross Talk through Complement Activation Modulates Amyloid Pathology in Mouse Models of Alzheimer ' s Disease. 2016; 36: 577–589.

Liddel SA, Guttenplan KA, Clarke LE, Bennett FC, Bohlen CJ, Schirmer L, et al. Neurotoxic reactive astrocytes are induced by activated microglia. *Nature* 2017; 541: 481–487.

Liguori R, Vincent A, Clover L, Avoni P, Plazzi G, et al. Morvan's syndrome: peripheral and central nervous system and cardiac involvement with antibodies to voltage-gated potassium channels. *Brain* 2001; 124: 2417–2426.

Meeker HC, Chadman KK, Heaney AT, Carp RI. Assessment of social interaction and anxiety-like behavior in senescence-accelerated-prone and -resistant mice. *Physiol. Behav.* 2013; 118: 97–102.

Patterson KR, Dalmau J, Lancaster E. Mechanisms of Caspr2 antibodies in autoimmune encephalitis and neuromyotonia. *Ann. Neurol.* 2018; 83: 40–51.

Piddlesden SJ, Jiang S, Levin JL, Vincent A, Morgan BP. Soluble complement receptor 1 (sCR1) protects against experimental autoimmune myasthenia gravis. *J. Neuroimmunol.* 1996; 71: 173–177.

Planagumà J, Leypoldt F, Mannara F, Gutiérrez-Cuesta J, Martín-García E, Aguilar E, et al. Human N-methyl D-aspartate receptor antibodies alter memory and behaviour in mice. *Brain* 2015; 138: 94– 109.

Sommer C, Weishaupt A, Brinkhoff J, Biko L, Wessig C, Gold R, Toyka KV. Paraneoplastic stiff-person syndrome: passive transfer to rats by means of IgG antibodies to amphiphysin. *Lancet.* 2005; 365: 1406–11.

Sonderen A Van, Ariño H, Petit-Pedrol M, Leypoldt F, Körtvélyessy P, Lancaster E, et al. The clinical spectrum of Caspr2 antibody – associated Neurology. 2016; 87: 521-8.

Sundal C, Vedeler C, Miletic H, Andersen O. Morvan syndrome with Caspr2 antibodies. Clinical and autopsy report. *J. Neurol. Sci.* 2017; 372: 453–455.

Viegas S, Jacobson L, Waters P, Cossins J, Jacob S, Leite MI, et al. Passive and active immunization models of MuSK-Ab positive myasthenia: Electrophysiological evidence for pre and postsynaptic defects. *Exp. Neurol.* 2012; 234: 506–512.

Wright S, Hashemi K, Stasiak L, Bartram J, Lang B, Vincent A, et al. Epileptogenic effects of NMDAR antibodies in a passive transfer mouse model. *Brain* 2015; 138: 3159–3167.

Xu W, Fitzgerald S, Nixon RA, Levy E, Wilson DA. Early hyperactivity in lateral entorhinal cortex is associated with elevated levels of A β PP metabolites in the Tg2576 mouse model of Alzheimer's disease. *Exp. Neurol.* 2015; 264: 82–91.

Zhao Z, Wang J, Zhao C, Bi W, Yue Z, Ma ZA. Genetic ablation of PLAG6 in mice leads to cerebellar atrophy characterized by purkinje cell loss and glial cell activation. *PLoS One* 2011; 6

Figure legends

Figure 1. Experimental design and selected behavioural tests. (A) Experimental design. The behavioural tasks assessed locomotion (open field, OF), strength (inverted screen, IS), coordination (accelerating rotarod, AR and narrow beam, NB), working memory (continuous spontaneous alternation, CSA), short- (forced alternation, FA) and long-term memory (novel object recognition, NOR - NORf, familiarization phase, NORf test phase), anxiety (light-dark box, LDb), compulsive-like behaviour (marble burying test, MB), social behavior (reciprocal social interaction tests, RSI) and olfaction (olfaction test, OT). (B) Representative images of cell-based assays showing CASPR2- Ab in the serum from a CASPR2-IgG injected mouse but not in the serum from a HC-IgG injected mouse (left panel). Blue = DAPI, green = eGFP, red = anti-human IgG. 63X, scale bar 10 μ m. (C) Continuous spontaneous alternations were reduced in CASPR2-IgG injected mice compared with HC-IgG injected mice ($P = 0.044$) but there was no difference in arm re-entries or in same arm re-entries. (D) In forced alternation, there were no differences in the preference index for number of entries or time spent in the novel arm (NA). (E) Novel object recognition test did not show differences between the two groups in the preference index for the novel object (NO) although there was a trend to reduced preference in CASPR2-IgG injected mice. (F) In the Reciprocal social interaction (RSI) test there was reduced latency to interact ($P = 0.04$; Mann-Whitney test) but no differences in the interaction time, or number of interactions. However, in the non-social aspects of the test, there was increased time spent immobile ($U = 0.008$), reduced rearing ($U = 0.02$) reduced grooming ($U = 0.018$) and longer duration of each grooming bout ($P = 0.002$). (H) The olfaction test showed no differences in the time spent or in the number of visits to the novel odor (NO). Data are expressed as mean \pm SEM with $N = 10$ for CASPR2-IgG injected and $N = 9$ for HC-Injected mice, with the exception of the RSI which was performed on 6 pairs.

Figure 2. Immunoglobulin G in the mouse brains and CASPR2 expression. (A) Representative images of IgG and CASPR2 expression in perfused fixed brains. 40X, scale bar, hippocampus 200 μ m, cerebellum 50 μ m. (B) CASPR2-IgG injected animals had higher levels of IgG in the cortex (Cx) ($P = 0.03$), hippocampus (Hip) ($P = 0.023$) and thalamus (Th) ($P = 0.0004$) compared to HC-IgG injected mice, but not in the cerebellum (Cb) ($N = 4/\text{group}$). No differences were observed in the levels of CASPR2 expression in the same areas (C) ($n = 4/\text{group}$). (D) Moreover, western blots of the whole brains from CASPR2-injected mice showed a trend towards increased CASPR2 expression compared to HC- injected mice (HC) (3 brains/group; means of $N = 4$ replicates for each brain). (E) Representative images of extracellular and intracellular CASPR2-IgG binding on hippocampal neurons dendrites (top), and graph (bottom) showing increase of intracellular puncta

density at 24 h ($P < 0.0001$) in CASPR2-IgG treated neurons without changes in extracellular binding. Scale bar 5 μm .

Figure 3. Effects of IgG on CASPR2-transfected HEK cells. A) Representative images (top) showing IgG in the cytoplasm (green) of HEK cells after 24 h incubation with CASPR2-IgG, without change of the membrane IgG binding (red), confirmed by profile plots (bottom) showing the mean fluorescent intensity for extracellular and intracellular IgG immunostaining across 13 cells. There was some IgG internalisation by 24h. Scale bar 10 μm . B) Representative FACS dot plot of IgG staining on CASPR2-IgG incubated cells (top). Each quadrant represents a cell subpopulation with relative percentages expressed as a number. A trend toward an increase of single stained intracellular (APC positive; top left quadrant) and double positive cells (PE and APC positive; top right) was observed over time along with a reduction of double negative (bottom left) and single stained extracellular cells (bottom right quadrant), particularly at 6 and 16 hours. C) MFI values of extracellular (top) and intracellular (bottom) IgG binding over time in cells incubated in CASPR2-Abs from 3 patients (the transferred and two others with very different CASPR2-Ab titres). No significant differences were detected, but there was a tendency towards an increase of extracellular and intracellular IgG over time. D) Representative FACS dot plot of commercial intracellular (APC) and extracellular (PE) CASPR2 staining on HC-IgG (top) and CASPR2-IgG (bottom) incubated cells. These cells showed no significant differences in the percentage of single intracellular (top left quadrant), double stained (top right quadrant), single extracellular (bottom right quadrant) and double negative (bottom left quadrant) cells. E) MFI values of membrane (top) and intracellular (bottom) CASPR2 staining in HEK cells incubated with HC (N=2) or CASPR2 (N=3) IgG or plasma. No differences were observed in extracellular or intracellular CASPR2 expression over time between the two groups. MFI = mean fluorescence intensity.

Figure 4. Analysis of neurons in mouse brains. (A) Representative pictures of NeuN expression and (B) quantification of NeuN positive cell densities in three brain regions. There were no differences between CASPR2-IgG and HC-IgG injected brains. (C) Calbindin expressing Purkinje cells (PC) were reduced in the cerebellum ($P=0.049$). (D) C-fos expression in the entorhinal-piriform cortex ($P=0.020$), dorsomedial hypothalamus (DMH) ($P=0.037$) and lateral hypothalamus (LH) ($P=0.031$) was higher in the CASPR2-IgG injected compared to the HC-IgG injected mice (Representative images are shown from the entorhinal-piriform cortex). N= 4 brains/group. 40X, 50 μm .

Figure 5. Microglial density and morphological analysis. (A) Representative images of the molecular layer of the cerebellum showing microglia staining. 40X, 20 μm . (B) CASPR2-IgG

injected mice showed higher microglia densities in the somatosensory cortex ($P=0.038$) and in the molecular layer (ML) ($P=0.002$) of the cerebellum but not in the granular layer (GL) or in the hippocampus. $N=4$ animals/group (C) Representative images of the z-stack projected IBA1 staining used for morphological analysis. 40X, 10 μm (D) Quantification of morphological data in the hippocampus and molecular layer of the cerebellum showed that microglia from CASPR2-IgG injected mice had a higher cell soma/cell total body size ratio and shorter ramifications than HC-IgG injected mice, compatible with an activated phenotype in both the hippocampus ($P=0.003$ and $P=0.010$, respectively) and the cerebellum ($P=0.0003$ and $P=0.008$, respectively). 200 cells from 4 animals/groups were analysed from the hippocampus and 100 from the cerebellar molecular layer.

Figure 6. Astrocyte morphology and inflammatory markers. (A) Representative images of GFAP staining in the molecular layer of the cerebellum and quantification of the mean fluorescence intensity in the same area showing higher GFAP expression in the CASPR2-IgG injected mice ($P=0.043$). $N=4/\text{group}$; 40X, 10 μm (B) Representative images of complement C3 expression on GFAP positive cells. Percentage of C3/GFAP area ratio per cell showed that increased C3 expression of astrocytes in the hippocampus ($t(398)=4.87$, $P<0.0001$, 200/cells from 4 animals/group), somatosensory cortex ($t(160)=2.41$, $P=0.01$, 81/cells from 4 animals/group) and cerebellum ($t(204)=7.14$, $P<0.0001$, 103/cells from 4 animals/group) of CASPR2-IgG injected mice. 40X, 10 μm (C) Representative pictures of the z-stack projected GFAP staining used for morphological analysis (40X, 10 μm). The astrocytes from CASPR2-IgG injected mice showed a smaller cell total body size ($U=22052$, $P=0.0051$, 228 cells from 4 animals/group) and shorter ($U=19946$, $P<0.0001$, 228 cells from 4 animals/group) maximal ramification length than HC-IgG injected mice, compatible with an activated phenotype, in the hippocampus. (D) Compared to HC-IgG injected mice, CASPR2-IgG exposed animals showed changes in several cytokines and chemokines, but none reached significance after correcting for multiple comparisons ($N=3/\text{group}$).

Behaviour and neuropathology in mice injected with human contactin- associated protein 2 antibodies

Running title: A passive transfer model of CASPR2 antibodies

Maria Pia Giannoccaro^{1,2}, David A. Menassa¹, Leslie Jacobson¹, Ester Coutinho¹, Gennaro Prota⁴, Bethan Lang¹, M Isabel Leite¹, Vincenzo Cerundolo⁴, Rocco Liguori^{2,5}, Angela Vincent¹

¹ Nuffield Department of Clinical Neurosciences, University of Oxford, Oxford, UK

² Department of Biomedical and Neuromotor Sciences, University of Bologna, Bologna, Italy

³ Biological Sciences, University of Southampton, Southampton, UK

⁴ MRC Human Immunology Unit, Weatherall Institute of Molecular Medicine, John Radcliffe Hospital, University of Oxford, Oxford, UK.

⁵ IRCCS Istituto delle Scienze Neurologiche di Bologna, Bologna, Italy

Correspondence

Prof Angela Vincent, Nuffield Department of Clinical Neurosciences, University of Oxford, Oxford, UK

Email angela.vincent@ndcn.ox.ac.uk

Tel 07817224849

Supplementary Material 15 pages, 3 figures

Methods

IgG purification and subclass analysis

The plasma from the CASPR2-Ab positive patient and the serum from the healthy donor were centrifuged, diluted 1:1 with Hartmann's solution and incubated with Protein G Sepharose column beads (Sigma-Aldrich, Inc.) overnight at 4 °C on a roller. The Sepharose-IgG mixture was then placed in a glass column before elution of IgG with 0.1M glycine solution (pH 2.3); the eluate was immediately neutralised with 1M Tris pH 8. The protein concentration of the elution was measured using a Coomassie Plus assay kit (Pierce, USA). The eluted fractions were pooled, dialysed against 2 l of Hartmann's physiological solution two times over 24 hours at 4 °C, concentrated by dialysis against polyethylene glycol and filter-sterilized. The concentration was determined using NanoDrop 3300 (ThermoScientific, UK), and IgG was stored at 4 °C.

For CASPR2 antibody subclass analysis, live human embryonic kidney (HEK) cells were incubated with serial dilutions of CASPR2-IgG for 1 hour (h) starting at 1:100 dilution at room temperature

(RT) and then fixed with 4% paraformaldehyde (PFA) in phosphate buffered saline (PBS). Binding of antibodies was detected by mouse anti-human IgG1 (Invitrogen, Thermo Fisher Scientific, #MH1013), IgG2 (#05-3500), IgG3 (#05-3600) or IgG4 (MA5-16716) (1:50) antibodies followed by goat anti-mouse IgG-Alexa Fluor® 568 (Thermo Fisher Scientific) conjugated secondary antibody (1:1000). Coverslips were mounted in mounting media (DAKO, Agilent, S3023) containing 4',6-diamidino-2'-phenylindole dihydrochloride (DAPI, Sigma Aldrich) (1:1000). A non-linear visual scoring system was used from 0 to 4. The dilutions of serum at which each subclass crossed the threshold of score 1 was used to calculate the proportion relative to the total.

Behavioural testing

Behavioural testing was done during the light phase. The animals were brought to the experimental room approximately 15 minutes before testing. A rest period of at least 2 hours was allowed between each test. Between mice the walls and the floor of the different apparatus were cleaned with 70% ethanol and dried with a dry tissue.

Accelerating rotarod (AR)

Accelerating rotarod was used to assess motor coordination (Deacon, 2013). The mice were placed on the rotating rod, facing away from the direction of rotation. The rotarod was initially set with a speed of 4 rpm for the initial 10 seconds after which an acceleration of 20 rpm/minute was applied. Time to fall was recorded. If the mouse had fallen off during the initial 10 seconds it would have another try, to a maximum of 3 trials.

Kondziela's inverted screen test (IS) or grip test

This test was used to assess muscle strength. The inverted screen consisted of a 43 caesurae of wire mesh consisting of 12 mm squares of 1 mm diameter wire, surrounded by a 4 cm deep wooden beading to prevent the mice from climbing to the other side. At the beginning of the test the mouse was placed in the centre of the apparatus on the under-side and the screen was quickly inverted while the timer was started. The inverted screen was held 50 cm above a padded surface for a maximum of 5 minutes. The time to fall was recorded. The average of three trials was taken as a final result.

Narrow beams (NB)

Narrow beams or static rods were used as another test of coordination (Deacon, 2013). For this test three wooden rods of varying thickness (35 (rod 1), 22 (rod 2) and 9 (rod 3) mm diameter) each 60 cm long were fixed to a laboratory shelf such that the rods horizontally protrude into space at an height of about 60 cm from a padded floor. The end of the rod near the bench has a mark 10 cm from the end, to denote the finishing line. The mouse was placed at the far end of the widest rod and the timer was started. The orientation time (time taken to orientate 180° from the starting position towards the shelf) and transit time (the time taken to travel to the shelf end) were recorded for a maximum of 5 minutes. If the mouse had not fallen and had arrived at the end of the rod, was transferred on the next smaller rod. If the mouse had not reached the end by this time the test was ended.

Marble burying test (MBT)

This test was used to assess the presence of repetitive, compulsive-like behaviors (Angoa-pérez et al., 2013). Standard polycarbonate mouse cages with fitted filter-top covers were fitted with fresh mouse bedding to a depth of 5 cm and its surface leveled by inserting another cage of the same size onto the surface of the bedding. Ten standard glass toy marbles (assorted styles and colors, 14 mm diameter) were placed on the surface of the bedding in two rows of five marbles. The mouse was placed into a corner of the cage containing the marbles and left undisturbed for 30 min. Food and water access was allowed during the test. At the end of the test the mouse was returned to its home cage and the number of marbles buried counted and expressed as percentage of the total. A marble was scored as buried if two-thirds of its surface area was covered by bedding.

Open field (OF)

The open field was used to assess motricity but also anxiety. The apparatus consisted of a dark closed arena of 50 x 50 cm divided into 10 cm squares illuminated with a 60 W lamp posed 45 cm above the centre of the floor of the box. The mouse was placed in a corner square facing the wall and its movement recorded on camera for 5 minutes. The latency to move, the number of peripheral and central square entered (four paws), the number of rears (both back paws on the ground but not part of grooming), the number of grooming and time spent grooming, the time spent in the peripheral and in the central squares, the time spent moving and the time spent freezing were recorded. The number of faecal boli and the presence/absence of urine were also recorded.

Light-dark box (LDb)

The LD box test was used to assess anxiety. The apparatus consisted of an open white compartment 30 x 20 x 20 cm joined by a 3 x 3 cm opening to a dark box 15 x 20 x 20 cm. The white compartment was illuminated by a 60 W lamp placed 45 cm above the centre of the floor. One side of the white compartment of the box was transparent allowing detection of the mouse movement. The mouse was placed in the middle of the light side facing away from the opening and a count-down timer for 5 min started. The latency to cross with all four paws to the dark side, the latency to cross with all four paws to go back for the first time to the light side, the total time spent on the light side and on the dark side and the number of transitions through the opening were registered for the test. The number of faecal boli and the presence/absence of urine were also recorded.

Forced alternation test (FA) or spatial preference test

This test was used as a measure of short-term memory. The apparatus was a Y-maze constructed from transparent Perspex and mounted on an opaque square Perspex board (64.5 cm x 56.5 cm). The walls of the Y-maze were 20 cm high and 0.5 cm thick. Each arm was 30 cm long and 8 cm wide. The test consisted of 3 periods: a habituation period (5 minutes), a delay period (1 minute) and a test period (2 minutes). During the exposure training trials the entrance to one arm (the Novel arm) was blocked using a rectangular piece of Perspex. The Novel arm was counterbalanced in each group between right and left side. At the start of a trial the mouse was placed at the end of the Start arm (which was always considered as the one closest to the experimenter) and allowed to explore the Start arm and the Other arm. During this period the time spent in each arm and the number of entries to each arm were recorded. An arm entry was defined as when a mouse had placed all four paws into an arm. At the end of the trial the mouse was removed from the maze and returned to its home cage for 1 minute during which the maze was cleaned and the block to the Novel arm removed. At the beginning of the test period the mouse was returned at the end of the Start arm and now allowed to explore the Start, Other, and Novel arms and exploratory behavior assessed for 2 minutes. During the test the time spent in each arm and the number of entries into each arm were recorded. Preference for the Novel arm was calculated as a Preference Index $(\text{entries/time in the new} - \text{entries/time in the old arm}) / (\text{entries/time in the new} + \text{entries/time in the old arm})$ for both the time in arms and number of arm entries (Rubovitch et al., 2010). Scores greater than 0.5 indicate a preference for the Novel arm.

Continuous spontaneous alternation (CSA) test

The continuous spontaneous alternation test was used as a test of working memory. The test was conducted in the same Y-maze as described above and it consisted of a single 5 min trial, in which the mouse was allowed to explore all three arms of the Y-maze. The start arm was varied between animals to avoid placement bias. Spontaneous alternation was assessed by scoring the pattern of entries into each arm during the 5 min of the test. Spontaneous alternation performance (SAP) was defined as successive entries into each of the three arms as on overlapping triplet sets (i.e., ABC, BCA, . . .) and scored as percent of spontaneous alternation (total alternations/total arm entries - 2*100) (Wietrzyk et al., 2005). The percentage of alternate arm re-entries (AARs) (i.e. ABA) and same arm re-entries (SARs) (i.e. AAB) were also scored for each animal in order to assess aspects of attention within spontaneous working memory (Wall and Messier, 2002). Total entries were scored as an index of ambulatory activity in the Y-maze.

Novel object recognition (NOR) test

The novel object recognition test was used to evaluate long term memory (Antunes and Biala, 2012). The open field arena was used in order to benefit from previous habituation. Towers of Lego bricks (X-cm high and X-cm wide) and Falcon tissue culture flasks filled with bedding (9.5 cm high, 2.5 cm deep and 5.5 cm wide, transparent plastic) were used as objects. Animals were randomly assigned one of those pairs of object for the familiarization phase. The test comprised two phases: a familiarization phase (NORf) and a test phase (NORt) performed 24 h later. During the familiarization session two identical objects (either towers of Lego bricks or Falcon tissue culture flasks; the pair was randomized to avoid preference bias) were placed in the open field arena, 5 cm away from the walls. The mouse was placed in the open field, its head positioned opposite the objects, and left free to explore for 5 minutes. The test phase was identical to the familiarization phase but one of the familiar object was replaced in the same position with a new object. The position of the novel object (left or right) was randomized between each mouse. The test was video recorded and subsequently analysed for number of visit and time spent with each object during both the familiarization and the test phase. The object exploration was scored whenever the mouse sniffed the object or touched the object while looking at it (i.e., when the distance between the nose and the object was less than 2 cm). Climbing onto the object (unless the mouse sniffs the object it has climbed on) or chewing the object did not qualify as exploration. If an animal had a total objects exploration time < 5 sec during any phase it was excluded from the analysis. The preference for the new object was expressed as Preference index [PI= (time new object - time familiar object)/(time new object + time familiar object)]. This result can varies from +1 to -1 with a positive score indicating preference for the novel object (Antunes and Biala, 2012).

Reciprocal social interaction test (RSI)

This is a social interaction test where two mice of the same treatment group, unknown to each other, are allowed to interact freely (Barkus et al., 2012). The apparatus was the same used for the open field as the mice were already habituated to it. Two animals from the same treatment group but housed in different cages, tightly matched for weight (within 5% difference) in order to avoid influences on the aggressive behaviour, were exposed to each other for 5 minutes. Six pairs per group were used. To meet the weight criteria one animal for each group was used twice. The test was video recorded and scored offline for the latency to start the interaction and for time spent in social and non-social behaviours and number of social and non-social events. Social behaviours included sniffing, grooming and following closely the other mouse; non-social behaviours included freezing, self-grooming (number of grooming and duration), and rearing.

Olfaction test (OT)

An olfaction test was performed in order to assess olfaction deficits that could interfere with the results from the social interaction test. The open field arena was used in order to benefit from previous habituation. A small plastic container with an odour (1 mL of vanilla or citrus food flavouring) was placed at two corners. The test comprised 3 phases: a sample phase (5 minutes), a delay period (5 minutes) and a test phase (5 minutes). During the first phase, the same odour was placed in both containers (half of the mice for treatment group would smell one odour, while the other half would smell the other). After this, the mice would return to the home cage for 5 minutes. During the test phase, a container with the alternate (new) odour was placed in one of the corners. The location of the new odour was counterbalanced across treatment groups. The test was video recorded and subsequently analysed for number of visit and time spent with each odour.

Ex vivo measurements

CASPR2 cell-based assays

Live cells were incubated with mice' sera for 1 hour (h) starting at 1:100 dilution at room temperature (RT) and then fixed with 4% paraformaldehyde (PFA) in phosphate buffered saline (PBS). Binding of antibodies was detected by goat anti-human IgG-Fc (1:750) (Thermo Fisher Scientific, # 31125) followed by donkey anti-goat IgG-Alexa Fluor® 568 (Thermo Fisher Scientific) conjugated secondary antibody (1:1000). Coverslip were mounted using mounting media (DAKO, Agilent, S3023) containing 4',6-Diamidine-2'-phenylindole dihydrochloride (DAPI, Sigma

Aldrich) (1:1000). A non-linear visual scoring system was used from 0 to 4; samples scoring ≥ 1 were considered positive. The end-point titre of positive samples was calculated by serial dilutions until the reactivity was no longer visible.

Morphological and immunofluorescence analysis of the brain and image processing

Perfused fixed brain sections were cut at 50 μm thickness using a Leica CM1900 cryostat in 10 series. Confocal images were taken of immunofluorescently labeled brain sections using a Zeiss LSM 710 confocal microscope and images were analysed with FiJi software (Open Source HR Software). Brightfield images were taken using the Aperio ScanScope (Leica Biosystem) and analysed in ImageScope (Leica Biosystem) .

Morphological measurements on brain tissue

The presence of gross morphological alterations was evaluated on Nissl-stained sections. Sections were mounted on super frost plus slides (vWR), left to dry at RT, fixed with 4% PFA for 10 minutes, rinsed twice in PBS and once in deionized water for 5 minutes and immersed in cresyl violet solution (Sigma C5042) for 10 minutes. Slides were then dehydrated by immersion in ethanol solutions of increasing concentrations until 100%, cleared with xylene and coverslipped with DPX mounting medium. Slides were scanned with the Aperio AT2 scanner and analysed with the e-pathology Aperio Imagescope image analysis system from Leica Biosystems. The sums of the area of a series of sections (12 sections), from the appearance of the frontal pole cortex to the most posterior part of cerebellum, was multiplied per the number of sections and the thickness of the section (50 μm) to obtain the total brain volume on the coronal plain. The same formula was used to calculate the cerebellum and hippocampus volumes (at least 4 sections). Thickness of the following structures were measured (25-50 measurements per area): anterior cingulate, motor, piriform and somatosensory cortices, neuronal layers of dentate gyrus, CA3 and CA1, CA4, CA3 and CA1 fields, granular and molecular layer of the cerebellum.

Immunostaining of brain tissue

Detection of IgG bound in vivo. To look at the similarity between CAPSR2 staining and IgG staining, two consecutive series were fixed with 4% PFA, washed 3 times in PBS, blocked for 1 h in PBS 10% normal goat serum (NGS) and incubated respectively with anti-human IgG antibodies (Biotium, USA, 20022, 1:500) and with rabbit monoclonal anti-CASPR2 antibodies (Abcam, EPR8738, ab137052, 1:500) in blocking solution overnight at 4°C. Two consecutive sections were

used to avoid any interactions between the secondary anti-human IgG and anti-CASPR2 antibodies. The day after, the sections were washed 3 times in PBS and incubated with goat anti-rabbit Alexa Fluor® 568 secondary (1:500) for 1 h at RT. All sections, including the one incubated with anti-IgG, were washed 3 times in PBS and coverslips were mounted using fluorescent mounting media containing DAPI (1:1000). For quantitative analysis of the mean fluorescent intensity, 32 single plain pictures (4 from the dentate gyrus, 4 from the CA3, 6 from the CA1 areas of the hippocampus, 6 from the somatosensory cortex, 6 from the thalamus, 6 from the cerebellum) were taken from 2 sections per animal. Mean fluorescence intensity was analysed with FiJi software (Open Source HR Software) and results plotted with GraphPad 6 as the mean of the intensity per each area per mouse.

Detection of subpopulations

Neurons and astrocytes were identified by immunofluorescence using a mouse anti-NeuN (Chemicon, MAB377; 1:500) and a polyclonal rabbit anti-glial fibrillary acidic protein (GFAP) antibody (Dako, Z0334; 1:500) respectively. Free-floating sections were fixed with 4% PFA, washed with PBS then blocked with 10% NGS in PBS-Triton-X-100 (0.3%) (PBS-T) for an hour then incubated overnight with primary antibodies at 4°C. The next day the sections were washed in PBS then incubated for two hours at RT with goat anti-mouse (568) and goat anti-rabbit (488) Alexa-fluor secondary antibodies from life technologies at 1:500 dilutions in blocking solution. Sections were subsequently washed in PBS, mounted on slides after a brief wash in TNS (pH = 7.4) and counterstained with DAPI mounting medium, left to dry then sealed and stored protected from the light at 4°C for confocal imaging. Cerebellar sections were stained similarly. In this case, however, primary antibodies included also guinea pig anti-calbindin D28K antibody (Millipore, AB1778; 1:200) for the identification of Purkinje cells. Secondary antibodies included goat anti-mouse (648), goat anti-rabbit (488/568), goat anti guinea pig (555). Neuronal and astrocyte cell densities were determined in the hippocampal fields (CA4, CA3, CA1), the somatosensory cortex and the piriform cortex. Confocal images were taken across the z-plane spanning the entire hippocampus in all cases in both hemispheres. Six images were taken per hemisphere for each cortical region. Eighteen stacks were taken every 2 µm z-plane for the hippocampus. For the neuronal density, cells were counted in every fifth image in the same stack. For astrocyte densities, images were z-projected and cells counted and the density calculated as number of cells per volume of area. In the cerebellum, confocal images were taken across the cerebellar lobules. Fifteen stacks were taken for each case every 3 µm z-plane. To avoid bias related to the different distribution of Purkinje cells across images the Purkinje cell density was calculated as linear density (number of calbindin positive cells per mm). At least 100 cells were counted for each case over 5.3 mm length.

Astrocytes density was assessed in the molecular layer of the cerebellum as mean fluorescence intensity of the GFAP staining. For the neuronal density in the molecular layer, images were z-projected on Fiji and NeuN positive cells counted.

Microglial cells were identified by the combined expression of IBA1 and CD68 markers. Free floating sections were fixed with 4% PFA, washed with PBS then blocked with 10% NGS in PBS-T 0.3% for an hour then incubated overnight with a rat anti-CD68 (BioRad, MCA1957; 1:400) and a rabbit anti-IBA1 (Wako chemicals, 019-19741) primary antibodies in blocking solution at 4°C. The sections were washed the next day with PBS-T 0.3% then incubated for two hours at room temperature with goat anti-rat (488) and goat anti-rabbit (568) Alexa-Fluor® secondary antibodies at 1:500 dilution in blocking solution in the dark. Sections were subsequently washed in PBS, mounted on slides after a brief Tris-NaCl solution (TNS) wash (pH = 7.4) and counterstained with DAPI mounting medium, left to dry then sealed and stored at -20°C for confocal imaging. Quantification of reactive microglia (defined as CD68/IBA-1 positive cells) was performed in the somatosensory and piriform cortex, the CA4, CA3 and CA1 fields of the hippocampus and in the granular and molecular layers of the cerebellum. For each hemisphere, seventeen z-stacks were taken in the hippocampus (3 for the CA4, 4 for the CA3 and 10 for the CA1), nine in the somatosensory area, 4 in the piriform cortex and 5 z-stacks per layer were taken in the cerebellum. The z-step/interval was 2 µm and microglial cells were counted within a 50 µm depth. An average density was obtained (cells/mm³) for each area.

Microglial morphology was assessed in confocal z-stacks detecting fluorescence on IBA-1 expressing cells in the hippocampus and in the molecular layer of the cerebellum as previously described (Coutinho et al., 2017). Soma size (µm²) and total cell body size (µm²) were measured and the soma/total cell body size ratio calculated and used as a marker of microglia activation. The length of the longest ramification (max ramification length) was recorded manually in Fiji.

For C-fos expression, free floating sections were rinsed in TNS, fixed with 4% PFA for 15 minutes then washed 3 times in PBS, blocked for one hour in 10% NGS 0.3% PBS-T and incubated with rabbit anti-cfos (Abcam, ab190289; 1:100) and mouse anti-NeuN (Chemicon, MAB377; 1:500) in blocking solution overnight at 4°C. The day after sections were washed and incubated with goat anti-rabbit (488) and goat anti-mouse (568) Alexa-Fluor® secondary antibodies at 1:500 dilution in blocking solution in the dark at room temperature for two hours. Sections were subsequently washed in PBS, mounted on slides after a brief TNS wash (pH = 7.4) and counterstained with DAPI mounting medium, left to dry then sealed and stored at -20°C for confocal imaging. Quantification

of cfos expressing neurons (defined as cfos/NeunN double-positive cells) was performed in the somatosensory, entorhinal and piriform cortex, the CA4, CA3 and CA1 fields of the hippocampus, the amygdala, the dorso-medial and lateral nuclei of the hypothalamus. For each hemisphere, twelve z-stacks were taken in the hippocampus (3 for the CA4, 4 for the CA3 and 6 for the CA1), four in the somatosensory area, 5 in the entorhinal-piriform cortex, 4 in the amygdala, and 4 z-stacks (2 per subarea) were taken in the hypothalamus. The z-step/interval was 2 μm within a 50 μm depth. An average density was obtained (cells/ mm^3) for each area.

Double staining for complement C3 fraction and GFAP was used to evaluate astrocyte activation. Free floating brain sections were mounted on Superfrost plus slides. When dry, sections were washed with TNS, immersed for 10 minutes in a boiled solution of citrate EDTA buffer and then left in the same solution for 20 minutes on ice. Sections were washed three times in PBS-T 0.3% and incubate with rat anti-C3 (Abcam, EPR19394, ab200999, 1:100) and rabbit anti-GFAP (Dako, 1:500) primary antibodies overnight at 4°C. The day after, sections were washed in PBS-T 0.3% and incubated with goat anti-rat (488) and goat anti-rabbit (568) Alexa-fluor secondary antibodies at 1:500 dilution in 5%NGS PBS-T 0.3% solution in the dark at room temperature for one hour. Slides were then washed in PBS-T 0.3% and TBS, counterstained with DAPI mounting medium, left to dry then sealed and stored at -20°C for confocal imaging. For each hemisphere, three z-stacks were taken in the hippocampus, somatosensory cortex and cerebellum at 40X magnification with a z-step of 2 μm within a 50 μm depth. Images were analyzed using Fiji. After z-projecting and automatic thresholding, the composed images were split in three channels. Images were magnified. Single astrocyte cells were manually selected, and for each cell the area on the GFAP and on the C3 channels measured. For each cells the C3 expression was calculated as C3/GFAP stained cell areas ratio. 200 cells/group were analyzed in the hippocampus, 81 cells/group in the somatosensory cortex and 100 cells/group in the cerebellum, and the results plotted as cells average/group average. Astrocytes morphology was assessed on the same z-stacks detecting fluorescence in GFAP expressing cells using the same script as for assessing microglia morphology (Countinho E et al 2017). The total cell body size (μm^2) was measured and the number of ramifications and the length of the longest ramification (max ramification length) were recorded manually in Fiji.

Cellular infiltration of B and T lymphocytes was assessed using rat anti-CD19 (Abcam, 1:100, ab25232) and rabbit anti-CD3 (Abcam, 1:100, ab16669) antibodies, respectively. Free floating brain sections were rinsed in TNS, fixed with 4% PFA for 10 minutes than washed 3 times in PBS, blocked for one hour in 10% NGS 0.3% PBS-T and incubated with primary antibodies in blocking solution overnight at 4°C. The day after sections were washed and incubated with goat anti-rat

(488) or goat anti-rabbit (568) Alexa-Fluor® secondary antibodies at 1:500 dilution in blocking solution in the dark at room temperature for one hour. Sections were subsequently washed in PBS, mounted on slides after a brief TNS wash (pH = 7.4) and counterstained with DAPI mounting medium, left to dry then sealed and stored at -20°C for confocal imaging.

Immunoblot and cytokine analyses

For total brain protein extraction, frozen brain tissue (3 brain and cerebellar hemispheres per mice/group) was homogenate in lysis buffer (50 mM TRIS-HCL, 150 mM NaCl, 0.1% SDS, 1% triton-X 100, pH 7.4) supplemented with protease inhibitors (1:100) with a mechanical homogenizer. The homogenate was then spun at 17000 rpm for 20 minutes at 4°C. Supernatant was collected and protein concentration measured by a Pierce™ BCA protein assay kit (23225).

For western blot (WB) analysis, NuPAGE sample reducing agent (10x; Invitrogen, NP0009) and LDS sample buffer (4x; Invitrogen,) were added to 10 to 30 µg of an appropriate amount of solubilized tissue, boiled for 10 minutes and the proteins separated into 3-8%Tris acetate SDS polyacrylamine gels (Invitrogen, NP0322) and transferred with dry blotting on nitrocellulose membranes. Membranes were blocked in 5% non-fat skimmed milk in PBS 0.1% Tween 20 solution and incubated overnight at 4°C with rabbit anti CASPR2 (Abcam, EPR8738, ab137052, 1:1000) and anti-GAPDH antibodies (Abcam, [EPR16891] ab181602 1:2000). Membranes were washed in PBS-Tween 0.1% and incubated with secondary antibodies in blocking solution for 1 h at room temperature (anti-rabbit IgG HRP 1:1000). Signals were detected by enhanced chemiluminescence (Amersham GE Healthcare) and captured on autoradiography film (GE Healthcare). All studies were done in duplicate or triplicate. Films were digitally scanned and signals quantified using Fiji ImageJ software. The signal intensity of each antigen was normalized to that of GAPDH in the same lane.

Brain cytokine expression was analyzed using a Mouse Cytokine Antibody Array (22 Targets) (Abcam, ab133993) as per manufacturer instructions. Briefly, membranes were blocked in blocking buffer for 30 minutes at room temperature then incubated with 250 of proteins from the brain lysate in blocking buffer overnight at 4°C. The day after, membranes were thoroughly washed and incubated with biotin-conjugated anti-cytokines antibodies overnight at 4°C. Following washing, streptavidin-HRP was applied for 2 hours at room temperature. Immunoreactivity was then visualized using enhanced chemiluminescence reagent. X-ray film was then scanned and densitometric analysis performed using Fiji. Positive controls were included on each membrane and

used for results normalization. The mean intensity of the normalized signal in HC-IgG injected mice was defined as 1 and the other intensities expressed relatively to this value.

In vitro studies on CASPR2 expression and internalisation in neurons and HEK cells

To evaluate the effects of CASPR2 antibodies in vitro, we initially assessed the presence of internalisation by evaluating surface and intracellular human CASPR2-IgG binding at time 0 and after 24 h rat hippocampal neurons and on transfected HEK cells by immunofluorescence analysis. Subsequently, transfected HEK cells were used to evaluate changes in CASPR2-IgG binding and CASPR2 expression over time using flow cytometry (FACS).

Hippocampal primary rat neurons (Kaech S and Banker G 2006) (DIV12) were incubated for 30 minutes or 24 h with either HC- or CASPR2-IgG (1:200) at 37°C, followed by washing and incubation with goat anti-human IgG 568 (1:1000) in blocking solution (1% BSA) for 30 minutes at RT. Coverslips were washed and fixed with 4% PFA and, after further washing, incubated with goat anti-human IgG 488 (1:1000) for further 30 min in PBS-0.3% triton, before mounting with DAPI. Confocal images were thresholded and analysed with SynPAnal software. For each image, 50 µm axonal segments were manually traced, and the puncta density automatically quantified for each segment.

HEK cells were transfected with CASPR2 cDNA. Sixteen hours after transfection, the media was replaced with media supplemented with either HC- or CASPR2-IgG (1:200). Cells were washed either 30 min (T0) or 24 h (T24) after exposure to the IgG and live cells immediately incubated with goat anti-human IgG 568 (1:1000) in blocking solution (1% BSA) for 30 minutes. Coverslips were washed and fixed with 4% PFA and, after further washing, incubated with goat anti-human IgG 488 (1:1000) for further 30 min in PBS-0.3% triton, before mounting with DAPI. Confocal photographs were taken at 63x magnification (10 fields/coverslip). Using ImageJ software, profile plots of each cell were made spanning the cell diameter for both the intracellular and the extracellular IgG immunoreactivity and the signal intensity was then averaged for the portion of the plot relating the membrane and for the one relating the cytoplasm.

For FACS, HEK cells were transfected with CASPR2-EGFP cDNA. Sixteen hours after transfection the media was replaced with media supplemented with either HC- (1 subject) or CASPR2- IgG (1 case) or plasma (2 patients with CASPR2 antibodies and 1 HC). Cells were washed either 30 min (T0), 6 (T6), 16 (T16) or 24 h (T24) after exposure to the IgG, detached and

seeded in V-bottom 96 well plates. Live cells were immediately incubated with goat anti-human IgG 568 (1:1000) in blocking solution (1% BSA) for 30 minutes or with mouse anti-CASPR2 (abcam, 1:200, 105581) followed by Alexa-Fluor goat anti mouse 568 for 30 minutes. Cells were washed, incubated 10 min with live/dead near infrared antibodies (Invitrogen), fixed with 4% PFA and, after further washing, incubated with either goat anti-human IgG 633 (1:1000) or with rabbit anti-CASPR2 (abcam, 1:200, ab33994) followed by goat anti-rabbit 647 for further 30 min in PBS-0.3% triton. After further washing cells were resuspended in PBS for flow cytometry cell acquisition. Compensation controls, i.e. unstained transfected HEK293 cells, were included in the analysis. Samples were acquired with a Fortessa X50 flow cytometer (BD biosciences), and analysed with FlowJo (Tree Star) gating on live cells. The percentage of cells stained only for APC (intracellular IgG) or PE (extracellular IgG) or for both (double positive) and the unstained (double negative) and the mean fluorescence intensity (MFI) for each time-point were analysed.

References

- Angoa-pérez, M. et al. (2013) 'Marble Burying and Nestlet Shredding as Tests of Repetitive, Compulsive-like Behaviors in Mice', (December), pp. 1–7. doi: 10.3791/50978.
- Antunes, M. and Biala, G. (2012) 'The novel object recognition memory: Neurobiology, test procedure, and its modifications', *Cognitive Processing*, 13(2), pp. 93–110. doi: 10.1007/s10339-011-0430-z.
- Barkus, C. et al. (2012) 'GluN1 hypomorph mice exhibit wide-ranging behavioral alterations', *Genes, Brain and Behavior*, 11(3), pp. 342–351. doi: 10.1111/j.1601-183X.2012.00767.x.
- Coutinho, E. et al. (2017) 'Persistent microglial activation and synaptic loss with behavioral abnormalities in mouse offspring exposed to CASPR2-antibodies in utero', *Acta Neuropathologica*. Springer Berlin Heidelberg, 134(4), pp. 567–583. doi: 10.1007/s00401-017-1751-5.
- Deacon, R. M. J. (2013) 'Measuring Motor Coordination in Mice', *Journal of Visualized Experiments*, (75), pp. 1–8. doi: 10.3791/2609.
- Kaech S, Banker G (2006). 'Culturing hippocampal neurons', *Nat Protoc*, 1(5), pp. 2406-15.

Rubovitch, V. et al. (2010) 'The intricate involvement of the Insulin-like growth factor receptor signaling in mild traumatic brain injury in mice', *Neurobiology of Disease*. Elsevier Inc., 38(2), pp. 299–303. doi: 10.1016/j.nbd.2010.01.021.

Wall, P. M. and Messier, C. (2002) 'Infralimbic kappa opioid and muscarinic M1 receptor interactions in the concurrent modulation of anxiety and memory', *Psychopharmacology*, 160(3), pp. 233–244. doi: 10.1007/s00213-001-0979-9.

Wietrzych, M. et al. (2005) 'Working memory deficits in retinoid X receptor γ -deficient mice', *Learning & Memory*, 12(3), pp. 318–326. doi: 10.1101/lm.89805.et.

Figure legends

Supplementary figure legends

Supp. Fig 1: Behavioral testing in mice exposed to HC- or CASPR2-IgG. All data are represented as CASPR2-IgG vs HC-IgG mean \pm SDs in the text but shown as mean \pm SEM in the Figures. A) Weights over time: no differences between HC and CASPR2-IgG injected animals (group $P = 0.83$, time \times status $P = 0.35$, repeated measure ANOVA). B) Accelerating rotarod (AR): no differences in the time to fall between groups ($t(17)=0.93$, $P=0.36$, unpaired t-test; 307.8 ± 150.3 vs 260.1 ± 27.9). C) Inverted screen (IS): no differences in time to fall between groups ($F(1,16) = 3.8$, $P = 0.06$, one-way ANCOVA; 227.3 ± 42.2 vs 269.6 ± 48.8). D) Narrow beam test, on the smallest beam: no differences between groups in orientation time ($F(1,17) = 0.03$, $P = 0.95$, two-way mixed ANOVA; 9.6 ± 7.9 vs 6.2 ± 3) or in transit time ($F(1,17) < 0.001$, $P = 0.98$, two-way mixed ANOVA; 63.9 ± 95 vs 49.7 ± 94.5). E) Marbles burying test (MB) no differences between groups in percentage of marbles buried ($F(1,16) = 0.52$, $P = 0.47$, one-way ANCOVA; 36 ± 24.1 vs 37.7 ± 21). F) Open field: no differences in number of central entries ($F(1,16) = 0.11$, $P = 0.73$, one-way ANCOVA; 4 ± 4 vs 5.1 ± 3.4), number of rearing ($F(1,16) = 2.53$, $P = 0.13$, one-way ANCOVA; 14.7 ± 15 vs 11.3 ± 6.4), number of grooming ($F(1,16) = 0.39$, $P = 0.54$, one-way ANCOVA; 2.9 ± 2.1 vs 2.4 ± 0.8) or time spent immobile ($F(1,16) = 1.1$, $P = 0.31$, one-way ANCOVA; 135.8 ± 48 vs 156 ± 51.4) between the two groups. G) Light-dark box: no differences between groups in latency to move to the dark side of the box ($F(1,16) = 1.05$, $P = 0.32$, one-way ANCOVA; 5.2 ± 2.4 vs 6.7 ± 3.4), time spent in the dark ($F(1,16) = 0.13$, $P = 0.71$, one-way ANCOVA; 268.3 ± 20.6 vs 267.4 ± 22) and number of crossings between the two chambers ($F(1,16) = 0.14$, $P = 0.71$, one-way ANCOVA; 7.6 ± 5 vs 7 ± 3.7).

Supplementary figure 2. Nissl staining. A) Photograph showing the cresyl violet staining of a brain serie (left panel) and volumetric measurements. No differences were observed in brain volume ($P=0.20$, unpaired t-test; 307.4 ± 34.7 vs 276.2 ± 7.7), cerebellar ($P=0.29$, unpaired t-test; 30.6 ± 3.9 vs 27.1 ± 3.1) and hippocampal volumes ($P=0.63$, unpaired t-test; 8.8 ± 0.99 vs 9.2 ± 1.2) between HC-IgG and CASPR2-IgG injected mice. B) Cortical thickness measurements. No differences were observed in the thickness of the anterior cingulate cortex ($P=0.80$, unpaired t-test; 751.6 ± 32.5 vs 758.9 ± 47.2), primary motor cortex ($P=0.91$; 1044 ± 115.7 vs 1036 ± 87.5), although a tendency towards a reduced thickness was noted in the piriform cortex of CASPR2-IgG injected animals compared to controls ($P=0.073$; 441.7 ± 20.8 vs 484 ± 33). C) Photograph showing an example of cortical layers measurement in the somatosensory cortex and quantification of the layers thickness. No differences were observed in the thickness of layer 1 ($P=0.46$; 87.2 ± 15 vs 76.3 ± 23.6), layers 2-4 ($P=0.83$; 406.6 ± 70.3 vs 415.2 ± 39.9) and layers 5-6 ($P=0.84$; 588.6 ± 78.4 vs 577.6 ± 77.5) between animals. D) Photograph showing an example of hippocampal cell body layers and fields measurements and their quantification. No differences were observed in the thickness of dentate gyrus (DG) ($P=0.96$; 63.5 ± 5.7 vs 63.4 ± 4.6), CA3 ($P=0.84$; 58.9 ± 3.4 vs 59.7 ± 5.4) and CA1 ($P=0.35$; 57.9 ± 5.7 vs 54.1 ± 8) nor in the thickness of CA4 ($P=0.56$; 192.7 ± 8.1 vs 183.3 ± 13.3), CA3 ($P=0.65$; 121.2 ± 16.3 vs 128.4 ± 34.7) and CA1 ($P=0.04$, not significant after Holm-Sidak correction for multiple comparison; 384.3 ± 32.7 vs 348.9 ± 17.4). E) Quantification of the thickness of cerebellar layers. No differences were observed between groups in the thickness of the granular ($P=0.70$; 145.9 ± 11.5 vs 150.4 ± 2.3) and molecular ($P=0.32$; 158.7 ± 8.6 vs 170.9 ± 12.9) layers of the cerebellum. Data are expressed as mean \pm SEM; $N=4$ brains/group.

Supplementary figure 3. Representative microphotographs of CD19 (top, green) and CD3 (bottom, red) staining in the parenchyma of CASPR2-IgG injected mice. Scale bar 20 μ m.